

VU Research Portal

Into the deep

Mulder, T.; Gillet, H.; Hanquiez, V.; Reijmer, J.J.G.; Droxler, A.W.; Recouvreur, A.; Fabregas, N.; Cavailhes, T.; Fauquembergue, K.; Blank, D.G.; Guiastrennec, L.; Seibert, C.; Bashah, S.; Bujan, S.; Ducassou, E.; Principaud, M.; Conesa, G.; Le Goff, J.; Ragusa, J.; Busson, J.

published in

Marine Geology

2019

DOI (link to publisher)

[10.1016/j.margeo.2018.11.003](https://doi.org/10.1016/j.margeo.2018.11.003)

document version

Publisher's PDF, also known as Version of record

document license

Article 25fa Dutch Copyright Act

[Link to publication in VU Research Portal](#)

citation for published version (APA)

Mulder, T., Gillet, H., Hanquiez, V., Reijmer, J. J. G., Droxler, A. W., Recouvreur, A., Fabregas, N., Cavailhes, T., Fauquembergue, K., Blank, D. G., Guiastrennec, L., Seibert, C., Bashah, S., Bujan, S., Ducassou, E., Principaud, M., Conesa, G., Le Goff, J., Ragusa, J., ... Borgomano, J. (2019). Into the deep: A coarse-grained carbonate turbidite valley and canyon in ultra-deep carbonate setting. *Marine Geology*, 407, 316-333. Advance online publication. <https://doi.org/10.1016/j.margeo.2018.11.003>

General rights

Copyright and moral rights for the publications made accessible in the public portal are retained by the authors and/or other copyright owners and it is a condition of accessing publications that users recognise and abide by the legal requirements associated with these rights.

- Users may download and print one copy of any publication from the public portal for the purpose of private study or research.
- You may not further distribute the material or use it for any profit-making activity or commercial gain
- You may freely distribute the URL identifying the publication in the public portal ?

Take down policy

If you believe that this document breaches copyright please contact us providing details, and we will remove access to the work immediately and investigate your claim.

E-mail address:

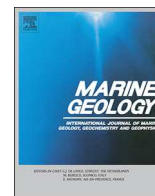
vuresearchportal.ub@vu.nl



ELSEVIER

Contents lists available at ScienceDirect

Marine Geology

journal homepage: www.elsevier.com/locate/margo

Into the deep: A coarse-grained carbonate turbidite valley and canyon in ultra-deep carbonate setting



T. Mulder^{a,*}, H. Gillet^a, V. Hanquiez^a, J.J.G. Reijmer^b, A.W. Droxler^c, A. Recouvreur^{a,f}, N. Fabregas^a, T. Cavailhes^a, K. Fauquembergue^a, D.G. Blank^c, L. Guiastrennec^a, C. Seibert^f, S. Bashah^d, S. Bujan^a, E. Ducassou^a, M. Principaud^a, G. Conesa^e, J. Le Goff^b, J. Ragusa^g, J. Busson^{a,h}, J. Borgomano^e

^a Université de Bordeaux-CNRS, UMR 5805 EPOC, Allée Geoffroy Saint-Hilaire, CS 50023, 33615 Pessac Cedex, France

^b College of Petroleum Engineering and Geosciences, King Fahd University of Petroleum & Minerals, Dhahran 31261, Saudi Arabia

^c Dept. of Earth, Environmental and Planetary Sciences, Rice University, 6100 Main Street, Houston, TX 77005, USA

^d CSL – Center for Carbonate Research, RSMAS, University of Miami, 4600 Rickenbacker Causeway, Miami, FL 33149, USA

^e Aix Marseille University, CNRS, IRD, Collège de France, CEREGE, Aix-en-Provence, France

^f Institut de Physique du Globe de Paris, Sorbonne Paris Cité, Université Paris Diderot, CNRS, 1, rue Jussieu, 75238 Paris Cedex 5, France

^g Section of Earth and Environmental Sciences, University of Geneva, 1205 Geneva, Switzerland

^h IFPEN, 1-4 avenue de Bois-Préau, 92852 Rueil-Malmaison, France

ARTICLE INFO

Editor: Michele Rebecco

ABSTRACT

New high-resolution multibeam mapping images detail the southern part of Exuma Sound (Southeastern Bahamas), and its uncharted transition area to the deep abyssal plain of the Western North Atlantic, bounded by the Bahama Escarpment extending between San Salvador Island and Samana Cay. The transition area is locally referred to as Exuma Plateau. The newly established map reveals the detailed and complex morphology of a giant valley draining a long-lived carbonate platform from its upper slope down to the abyssal plain. This giant valley extends parallel to the slope of Long Island, Conception Island, and Rum Cay. It starts with a perched system flowing on top of a lower Cretaceous drowned main carbonate platform. The valley shows low sinuosity and is characterized by several bends and flow constrictions related to the presence of the small relict isolated platforms that kept alive longer than the main platform before drowning and merging tributaries. Turbidite levees on either side of the valley witness the pathway of multiple gravity flows, generated by upper slope over steepening around Exuma Sound through carbonate offbank transport, some of them locally $> 15^\circ$, and resulting slumping. In addition, additional periplatform sediments are transported to the main valley through numerous secondary slope gullies and several kilometre-long tributaries, draining the upper slopes of cays and islands surrounding Exuma Plateau. Some of them form knickpoints indicating surincision of the main Exuma Valley which is consistent with an important lateral supply of the main Exuma Valley. Prior to reaching the abyssal plain, the main valley abruptly evolves into a deep canyon, 5 km in width at its origin and as much as 10 km wide when it meets the abyssal plain, through two major knickpoints named “chutes” with outsized height exceeding several hundred of meters in height. Both chutes are associated with plunge pools, as deep as 200-m. In the deepest pools, the flows generate a hydraulic jump and resulting sediment accumulation. When the canyon opens to the San Salvador abyssal plain, the narrow, deep, and strong flows release significant volume of coarse-grained calcareous sediments in numerous turbidite layers interbedded with fine mixed siliciclastic and carbonate sediments transported by the Western Boundary Undercurrent (WBUC) along the Bahama Escarpment. Carbonate gravity flows exiting the canyon decelerate at the abyssal plain level and construct a several-kilometre-wide coarse-grained deep-sea turbidite system with well-developed lobe-shape levees, partially modified by the flow of strong contour-currents along the Bahama Escarpment.

* Corresponding author.

E-mail address: thierry.mulder@u-bordeaux.fr (T. Mulder).

<https://doi.org/10.1016/j.margeo.2018.11.003>

Received 30 May 2018; Received in revised form 22 October 2018; Accepted 3 November 2018

Available online 07 November 2018

0025-3227/ © 2018 Elsevier B.V. All rights reserved.

1. Introduction

Large turbiditic systems have been extensively studied in siliciclastic environments including both outcrops and modern analogues, such as the modern sand-rich Navy Fan (Normark et al., 1979), the mud-rich Congo-Zaire system (Droz et al., 1996), or the ancient Annot Sandstone systems (Joseph and Lomas, 2004). Various classifications were proposed using the source type (Reading and Richard, 1994) or the geodynamic context (Shanmugam et al., 1988).

In carbonate environments, early models (Cook and Egbert, 1981) were directly influenced by siliciclastic fan models (Normark, 1970; Mutti, 1977). The slope apron model (Schlager and Chermak, 1979; Mullins and Cook, 1986) represents an extent of the debris-sheet model of Cook et al. (1972) but remains too much restrictive as it does not reflect the complexity of carbonate slope systems and does not include all the architectural elements (Miall, 1985) that become progressively evidenced by improved multibeam mapping technologies. The calciclastic submarine fan model (Payros and Pujalte, 2008) defines three fan types that take into account tectonic heritage and dominant particle grain size. It fits with numerous case studies both on rock outcrops and modern analogues but needs to be tested with the Bahamian case study we present in this paper. In siliciclastic environments, the system can be a point source, linear source or multiple sources (Reading and Richard, 1994). In prevalent carbonate environments, the sediment transfer from the platform upper slopes towards the basin was thought to form a line source rather than a point-sourced fan accumulation, and hence would not challenge the size of their siliciclastic counterparts (Shanmugam et al., 1988; Playton et al., 2010; Reijmer et al., 2015a). This idea relies on a series of studies from various Bahamian slopes and basins, e.g. the Columbus Basin (Bornhold and Pilkey, 1971), the Tongue of the Ocean (Schlager and Chermak, 1979; Droxler and Schlager, 1985; Haak and Schlager, 1989), Exuma Sound (Crevello and Schlager, 1980; Droxler, 1984; Droxler et al., 1988; Reijmer et al., 1988, 2012, 2015b) and on the upper slope of Little Bahama Bank (LBB; Mullins et al., 1984). Modern turbidite systems on the LBB slope include small canyon-lobe systems (Mulder et al., 2012; Tournadour, 2015). Although it is intuitively accepted that the observed, large, and well-developed Bahamian Canyon systems had to be generated through erosion by numerous gravity flows generated during the transfer of neritic carbonate sediment from the platform upper slope into the abyssal plain, systematic imaging of those canyons using high-resolution multibeam mapping was not achieved so far.

The study the Exuma Canyon system includes (1) the southeastern extremity of Exuma Sound, (2) the Exuma Plateau, defined as the area bounded by Crooked Island in the south, Samana Cay in the southeast, Conception Island and Rum Cay in the north, Long Island in the west and the Bahama Escarpment in the east, and (3) the San Salvador Abyssal Plain, immediately at the basis of the Bahama Escarpment (Fig. 1). The newly acquired detailed bathymetric maps and a high-resolution seismic grid were tied with ODP leg 101, sites 631, 632, and 633 (Austin et al., 1996, 1988) in the southeastern extremity of Exuma Sound. The newly acquired bathymetric and seismic surveys of the Exuma Plateau reveals in great details a giant and wide valley, fed by numerous tributaries and gullies, evolving into a deep canyon, 5 km in width at its origin and as much as 10 km wide before it meets the San Salvador abyssal plain. This study provides new information on the sediment transfer from the upper slopes of southern Exuma Sound at a few hundreds of meters into the San Salvador Abyssal Plain deeper than 4500 m in water depth. The San Salvador Abyssal Plain is bounded on its western and southern sides by the 1200-km-long Bahama Escarpment, an impressive, 1000 to 2000 m high, steep submarine cliff with slopes reaching up to 40° (Freeman-Lynde et al., 1981; Freeman-Lynde and Ryan, 1981) constructed by Early Jurassic to Early Cretaceous limestones (Schlager et al., 1984).

The presence of convex-bankward embayments at the platform edge, in particular in southeast Bahamas and along the Bahama

Escarpment (called Blake Escarpment when bordering the Blake Plateau or sometimes the Blake-Bahama Escarpment), has been interpreted as erosional features and led Mullins and Hine (1989) to define the “scalped bank margin” as the result of intense carbonate platform disintegration. Both large-scale mass-wasting processes and undercutting/dissolution by deep-water currents (Paull and Dillon, 1980) could be at the origin of this erosion and would be responsible of the ca. 5 km retreat of the Bahama Escarpment (Freeman-Lynde et al., 1981; Freeman-Lynde and Ryan, 1981; Schlager et al., 1984). Using rock samples collected by dredging and ages of Neptunian dykes, Corso (1983) suggests that this escarpment already existed by the Late Cretaceous. The toe of this escarpment at 4000 and 5000 m is currently bathed by the Western Boundary Undercurrent (WBUC; Bulfinch et al., 1982), which consists of the lower part of the south-flowing western boundary current of the North Atlantic Deep Water. Velocity peaks of up to 70 cm s⁻¹ have been measured for this current (Heezen and Hollister, 1971), therefore strong enough to transport a large volume of fine siliciclastic clayey sediment into the San Salvador Abyssal Plain sourced as far north as the Canadian Maritime Provinces (Fig. 1A; Droxler, 1984; Cartwright, 1985). At greater water depths, the upper part of the Antarctic Bottom Water flows northward.

These large-scale embayments could finally represent a first step in the formation of larger scale reentrant defined by Schlager et al. (1984) that represent intra platform basins dissecting Great Bahama Bank.

Few studies in the 1980's were conducted in our study area. They focused on the late Quaternary sedimentation patterns in Exuma Sound (Crevello and Schlager, 1980; Droxler, 1984), the seismic interpretation of the Exuma Plateau (Schlager et al., 1984; Corso, 1983), and in the vicinity of the Bahama Escarpment, Ladd and Sheridan (1982, 1987) recognised some deep structures and faults displacing the earlier Bahama Platform.

Crevello and Schlager (1980) described gravity-displaced carbonate sediments in the northwest part of Exuma Sound, including debrites, mud and grain flow deposits, and turbidites containing 50–70% of neritic skeletal and non-skeletal grains and fragments in addition to lithoclasts and intraclasts derived from the neighbourhood platforms, the rest consisting of planktonic foraminifers essentially and pteropods. The largest turbidite layer with a more restricted debris flow basis in surface area extends across almost the whole Exuma basin (6400 km²), representing a volume > 10⁸ km³. Two smaller turbidite layers form lobate, pinching downslope geometries extending 10–15 km into the Exuma seafloor. The debris flow crossed the full length of Exuma Sound axis (100 km) before to be channelled into the broad Valley on the Exuma Plateau. ODP Leg 101 core analyses at Sites 631 to 633 allowed to link Quaternary cyclic bank sediment export to successive surrounding bank top flooding sand exposure related to interglacial/glacial sea-level fluctuations (Droxler et al., 1988; Reijmer et al., 1988), particularly using aragonite cycles for the late Quaternary in Tongue of the Ocean (Droxler, 1984; Droxler and Schlager, 1985). Other studies focused on the compositional variations of carbonate gravity deposits and linked those to sea level dependent sediment export (Reijmer et al., 2012, 2015b) and carbonate platform margin transitions (Reijmer et al., 1992).

The Exuma Plateau consists of a thick sedimentary pile of Kimmeridgian-Oxfordian limestones overlain by upper Jurassic to lower Cretaceous chinks and dark Aptian to Cenomanian carbonate mud typifying the drowning of the platform. This drowned Mesozoic carbonate platform is now covered by Cenozoic periplatform oozes that are particularly well developed in the southern part of Exuma Plateau. The abyssal plain is formed by a basaltic substratum that corresponds to the top of the oceanic crust.

Prior to the 2016 cruise on R/V L'Atalante, the broad valley evolving into a narrow deep canyon in the Exuma Plateau was barely imaged in the BACAR survey. Mullins et al. (1982) interpreted the Great Abaco Canyon, located north of the Little Bahama Bank, as potential analogue with the wide valley/deep canyon in Exuma Plateau, formed

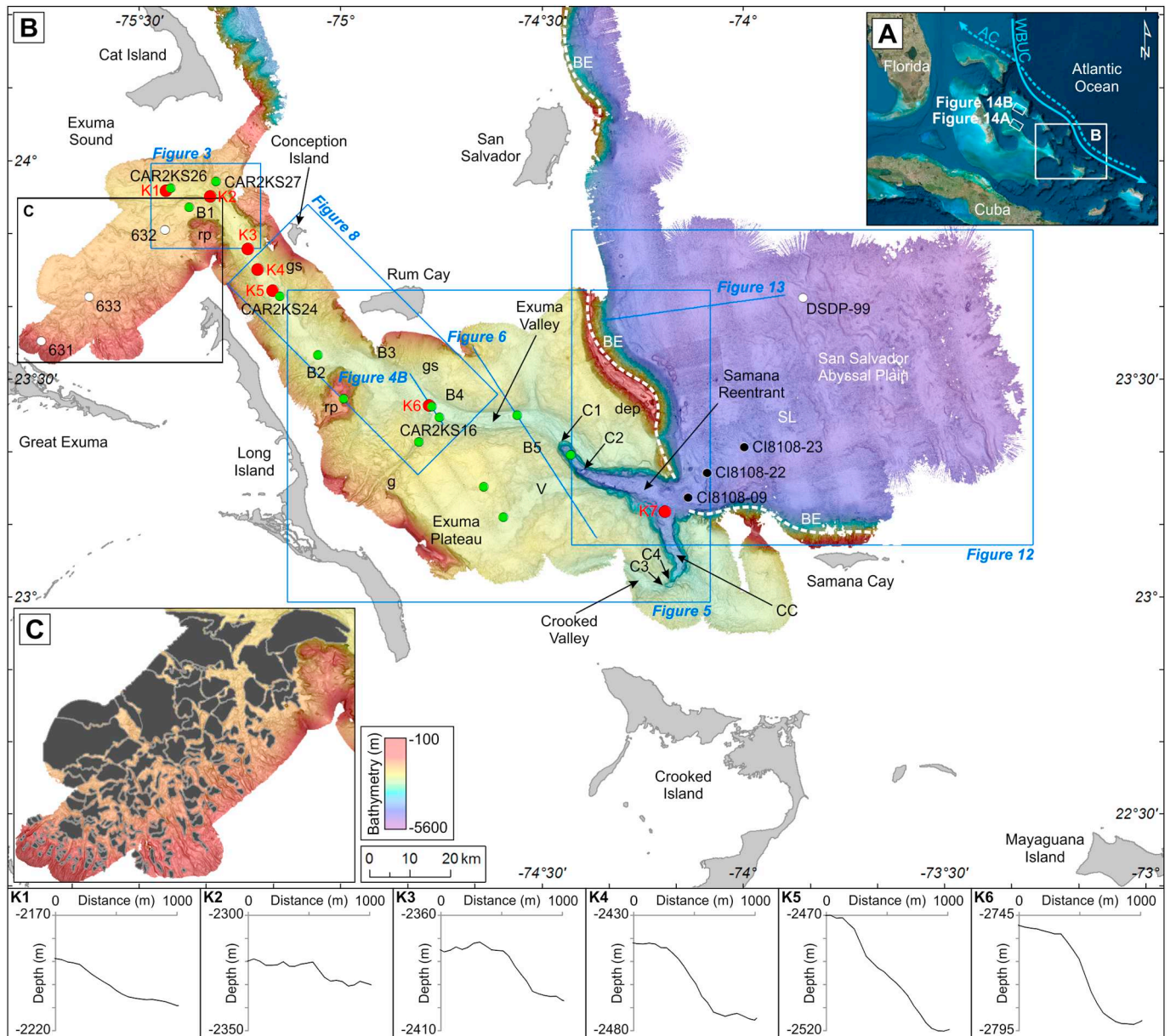


Fig. 1. (A) Location map of the study area. Blue arrows indicate trajectories of the main oceanic currents in the western part of the Bahamian archipelago. AC: Antilles Current (dash line). WBUC: Western Boundary Undercurrent (plain line). (B) Bathymetric map of the study area ranging from the south end of Exuma Sound to the San Salvador Abyssal Plain. B1–B5: bends; BE: Bahama Escarpment; C1–C4: Chutes; CC: Crooked Canyon; CC: Crooked Valley; dep: drowned elongated platform; g: major gully; gs: gullied slope; K1–K7 knickpoints; rp: Relict platform; SL: Sedimentary Levee; V: Large valley tributary of Exuma Valley in the South of Exuma Plateau; White dashed line indicates the top of the Bahama Escarpment. Red dots represents knickpoints location. Green dots represent Carambar 2 core locations. White dots are ODP/DSDP wells 631, 632 and 633. Insets: Longitudinal cross-section through knickpoints K1 to K6. C: Enlargement of the bathymetric map of the south-east toe of the slope of Exuma Sound showing sediment-filled slump scars (dark-grey tone). (For interpretation of the references to color in this figure legend, the reader is referred to the web version of this article.)

prior to Santonian along a zone of structural weakness, the Great Abaco Fracture Zone. The canyon enlarged and deepened because of wall accretion combined with subsidence (until Campanian) and also as a consequence of sporadic and episodic erosional downcutting by mass-flow processes (Mullins et al., 1982). One among the many results of the BACAR cruises, according to Ravenne et al. (1985) and Ravenne (2002), was the occurrence of a coarse-grained turbidite system interpreted as a sedimentary levee build along the Bahama Escarpment in the San Salvador Abyssal Plain. The study suggests distal supply of bank top derived calcareous sands by Exuma Canyon (and a local source from the Bahama Escarpment generating mass-flow deposits containing Cretaceous flintstone). The turbidite system forms a biconvex lens, 10 km long and about 1000 m thick (Ravenne, 2002). Correlation with

DSDP boreholes 99, 100, 101 and 391 (Hollister et al., 1972; Benson et al., 1978) located to the east of the Blake Plateau scarp allowed to distinguish three sequences, i.e. Upper Cretaceous, Neogene, and Quaternary. The analyses of the 13 cores collected during the BACAR cruise in the San Salvador abyssal Plain identify coarse carbonate gravity flow deposits, including debrites, no- to poorly-graded hyperconcentrated and concentrated flow deposits as well as normally-graded turbidites s.s. (Fig. 2). These gravity flow deposit layers are intercalated with dark clay-rich beds, based upon their mineralogy originating from the Canadian Provinces and transported by the WBUC forming well-defined contourites (Fig. 1; Droxler, 1984; Cartwright, 1985; Schmitt, 2013).

The current study investigates the morphological expression of a

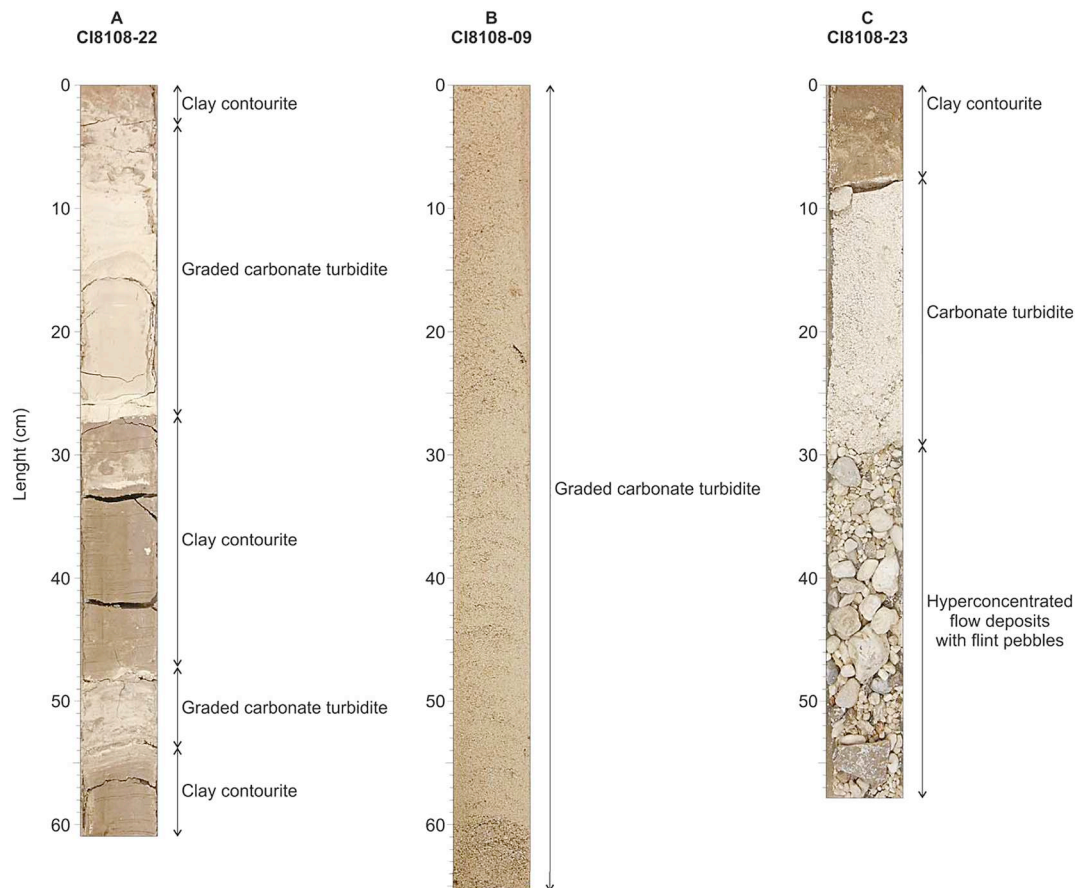


Fig. 2. (A) BACAR core CI8108-22 showing the alternation of fine-grained grey carbonate turbidites and dark clay contourites (Cartwright, 1985). (B) BACAR core CI8108-09 showing a carbonate turbidite (Cartwright, 1985). (C) BACAR core CI8108-23 showing a coarse-grained mass-flow deposit including siliciclastic pebbles and a calcarenitic turbidite (Cartwright, 1985). See Fig. 1 for core location.

large-scale sediment transfer from a carbonate platform upper slopes of a perched basin into the abyssal plain. It reveals a series of sedimentary morphologies, in particular the coarse-grained deep-sea carbonate turbidite system and encountered sediment sources and transport processes of this intra-platform basin drainage system. Finally, the study shows that, if the presence of these deep incisions is probably related to tectonic-oriented erosion, mass-flow processes (sensu Mulder and Alexander, 2001) including turbidity current activity have been underestimated in shaping the present-day canyon morphology.

2. Methods and acquired data

Leg 2 of the CARAMBAR 2 cruise was conducted from December 20, 2016 to January 2, 2017 onboard the R/V *L'Atalante*. The survey used a Kongsberg EM122/EM710 multibeam echo-sounder (bathymetry and backscatter), a very-high resolution (“Chirp” sub-bottom profiler) with 1800–5300 Hz frequency modulation, a high-resolution (HR) multi-channel seismic system (four 35/35 cu in GI air guns and a 192 channel streamer), and a Kullenberg coring system. Data collected included 20,395 km² of multibeam bathymetry and backscatter, 2149 km of HR seismic profiles (penetration 1–2.5 s two-way travel time), and 13 cores with a total length of 83 m (Fig. 1). These new data sets from the southern part of Exuma Sound, Exuma Plateau, and adjacent San Salvador Abyssal Plain, complement the existing data in this area. These include academic and industrial seismic lines, bathymetry and cores provided by the BACAR cruises (Ravenne et al., 1985; Ravenne, 2002) which, among other objectives, focused on the San Salvador Abyssal Plain first bathymetric maps and late Quaternary sediment accumulation (Droxler, 1984; Cartwright, 1985). It also comprises the results of

Ocean Drilling Program Leg 101 (Austin et al., 1996, 1988) and regular piston core studies (Crevello and Schlager, 1980; Droxler, 1984; Cartwright, 1985) as well as the interpretation of a seismic line crossing the San Salvador Abyssal Plain from DSDP Site 99 through Exuma Canyon located in the southern part of Exuma Plateau (Schlager et al., 1984).

3. Results

3.1. Perched slope basin, southern Exuma Sound

Exuma Sound is a U-shaped, intra-platform basin deepening towards the southeast from 1200 to 2000 m. Our survey is restricted to the southeastern part of the basin covering the area near ODP sites 631, 632, and 633 (Fig. 1A). South of Exuma Valley, the slope bordering the Great Exuma and Long islands shows a hummocky morphology with numerous topographic depressions extending perpendicular to the slope and limited upslope by a sub-vertical wall. These depressions have a ca. 2–3 km spacing on the slope (Fig. 1A and C). They become less frequent and with a larger spacing of ca. 5 km in the basin. The slopes of Great Exuma and Long islands in Exuma Sounds are crossed cut by > 30 gullies as shown on the bathymetric map collected in this study (Fig. 1A and C). Most of them are 5–15 km long and initiate along Great Exuma Island where slopes reach 15° in the southwestern part and decrease to 5–10° in the northeastern part (Fabregas, 2018). In the southern part of Exuma Sound and on the adjacent Exuma Plateau, Exuma Valley is only 400 m deeper than the mean seafloor of the Exuma Plateau and 8 km wide. South of Cat Island, this valley bends when exiting Exuma Sound (B1 in Figs. 1B and 3) to restrict its location

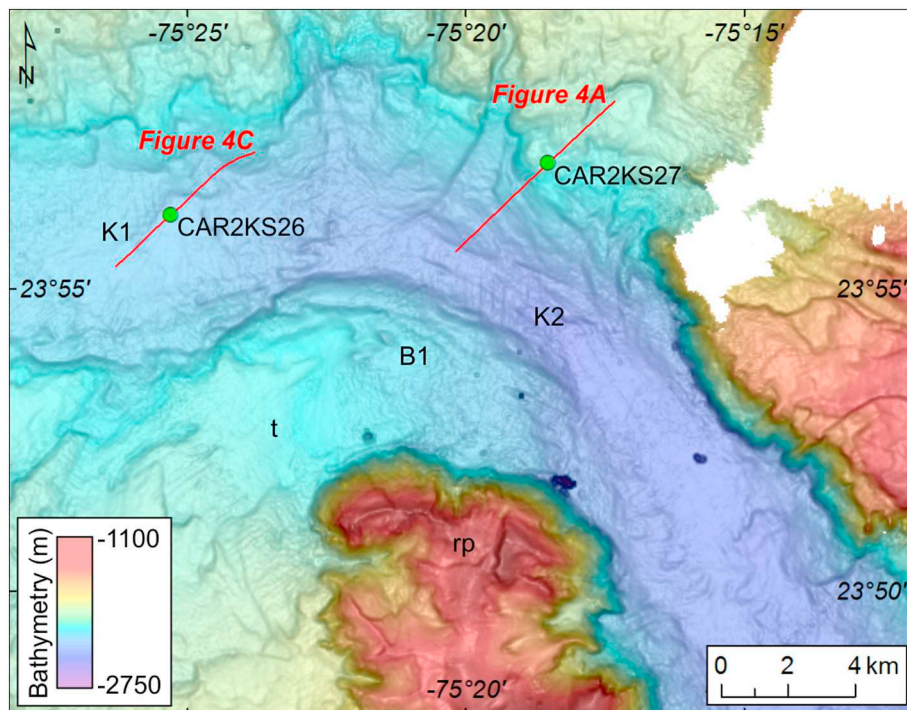


Fig. 3. Enlargement of the bathymetry showing knickpoints K1 before bend B1 and K2 at the output of bend B1, the terrace (t) developed on the internal side of the bend and location of very-high resolution seismic profiles in Fig. 4A and C. Note the presence of relict platform (rp). See Fig. 1B for profile location.

between the northern partially drowned parts of the two Long and Conceptions Island platforms that remained active until the Quaternary. At this bend location (B1), the Valley width decreases to 4.5 km, and is associated with a 25-m-thick knickpoint (K2 in Fig. 3). The axis of Exuma Valley is covered with a high-amplitude surface reflector laying above a blind echofacies. Core CAR2KS26 collected at this location (Fig. 4C) shows block-rich deposits at its base (from 350 to 304 cm) followed by a poorly graded sequence (between 304 and 252 cm), then by a well-graded fine-grained sequences (between 252 and 195 cm) and finally by an inversely-graded, laminated sequence (between 195 and 167 cm; Fig. 4E). On the south (internal) part of the bend, a flat elongated terrace can be observed (t in Fig. 3). Very-high resolution seismic profiles at this location show layered echofacies with high/low acoustic impedance alternations suggesting “moustache shape structures” (Fig. 4A). Core CAR2KS27 was collected in this layered echofacies. It shows several fining-up sequences with coarse carbonate sand (Fig. 4D left) or fine sand (Fig. 4D right) at the base and carbonate mud at the top. The Exuma Valley shows an additional constriction just at the southeastern mouth of Exuma where it is confined between the slope of Conception and an isolated topographic high bordering Long Island (rp in Fig. 1).

3.2. Exuma Plateau

Exuma Plateau is a gently dipping deep-water platform trending southeast with a mean slope $< 0.4^\circ$ if excluding the isolated topographic highs (rp in Figs. 1 and 5) and the Exuma Valley. If one look at the elevations of the drowned parts of this large platform, such as the northern part of Long and Conception Islands and the Bahama Escarpment and unnamed platforms in Figs. 3 and 5, one could argue that the top of the large platform has remained relatively sub horizontal. The drainage network within the Exuma Plateau shows that the main Exuma Valley is fed by a dense well-organized dendritic network of gullies systematically draining slopes surrounding and topographic highs topographies within Exuma Plateau (Fig. 5). On a seismic line crossing Exuma Valley, almost perpendicularly to its axis (Fig. 1) the

valley displays a U-shaped cross section (Fig. 6). The seismic facies (Fig. 6) show a first unit at the base of the profile constituted with parallel, medium amplitude reflectors. It is overlain by a thinner second unit with very-high amplitude reflector and an irregular top topography. The third unit shows mid-amplitude, sometimes discontinuous reflectors sometimes affected by erosional surfaces. The axis of Exuma Valley within Exuma Plateau, with a mean slope of approximately 0.4° , forms four bends (B2 to B5 in Fig. 1B). Some of these bends (B1 and B2/B3) seems strictly constrained by the drowned topography of the main carbonate platform. Along Long Island, Conception Island and Rum Cay, Exuma Valley pathway is constrained by the steep slopes bordering the islands. An isolated topographic high located between Long Island and Rum Cay lays some 1100 m above the surrounding seafloor (rp in Figs. 1A, 5, 7A). It shows at its top some “ridges” or better higher topographies on its north and western margins. Another 40 km long positive topography (1100 m to 1800 m high) extends along the edge of the modern Bahama escarpment (dep in Figs. 1A and 7B). The edges of these topographic highs or small keep up drowned platforms, are affected by numerous scars and gullies draining their steep margins (Fig. 7). The flanks of Exuma Valley show also abundant scars suggesting numerous sediment failures, particularly on the northern side (Fig. 8). In addition to these scars several smaller gullies drain the slopes of Conception Island and Rum Cay, before merging with Exuma Valley (gs in Figs. 1A and 8). These small gullies in some instances evolved at their terminus into small lobate bulges (lb in Fig. 8). Some of these gullies merge with the main Exuma Valley just after a ca. 30 m-thick knickpoint (K3, K4, K5; Fig. 1) On the southwest side, the valley is also connected to large gullies (g in Figs. 1B and 8). The longest one extends over 30 km and comes from the upper slope of Long Island. It incises the canyon floor forming a little 50-m-high knickpoint just up-slope of the junction (K6 in Figs. 1B and 8). At this location, very-high resolution seismic profiles show “moustache shape structures” consisting of layered echofacies with high/low acoustic impedance alternations (Fig. 4B).

Further down the Exuma Valley, the seafloor is covered by large symmetrical undulations with a height of 20 m and a wavelength of

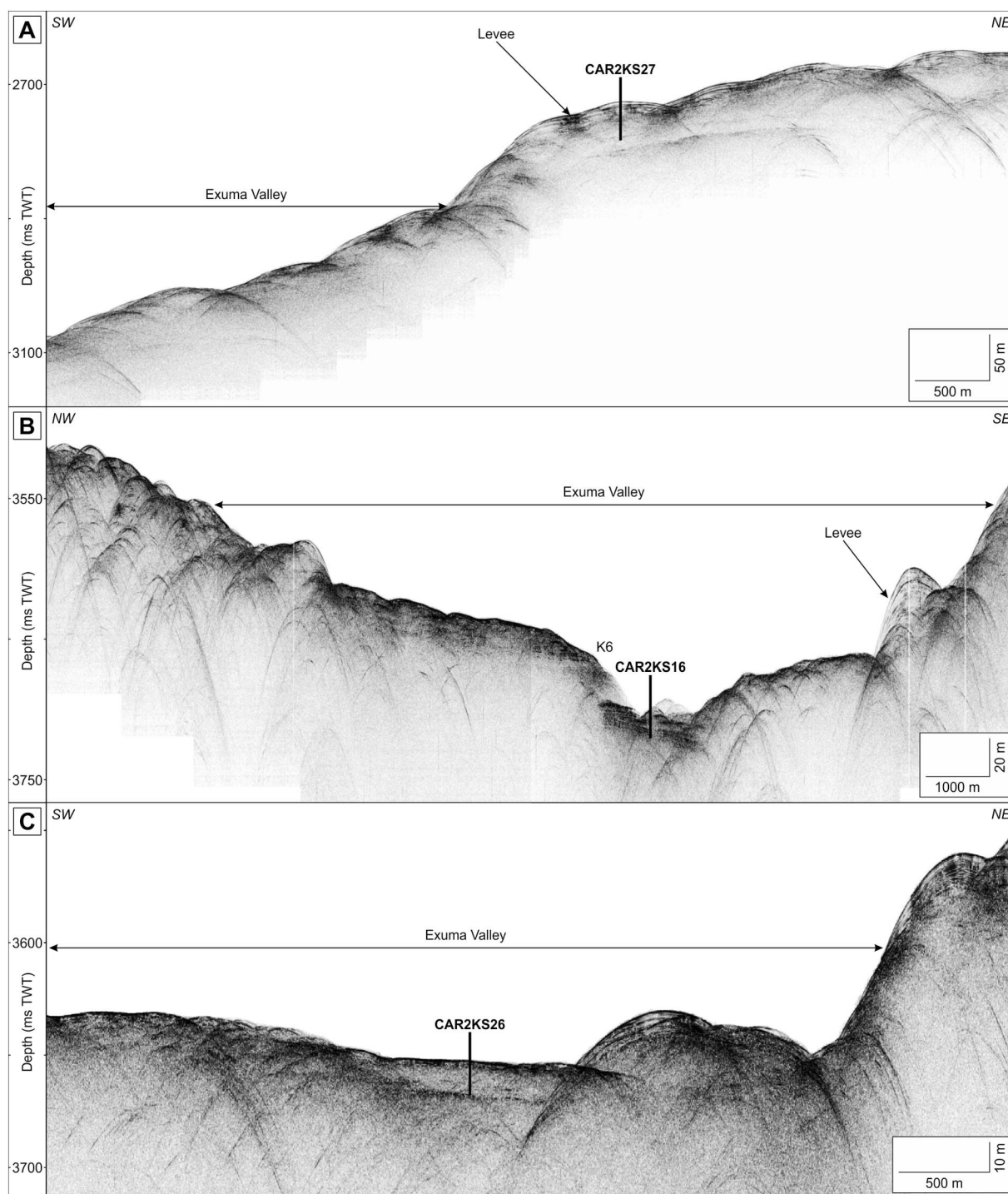


Fig. 4. Very-high resolution seismic (Chirp) profiles showing layered echofacies interpreted as levee deposits at the mouth of Exuma Sound (A), between bends B3 and B4 in Exuma Valley (B) and in the Exuma Valley (C). See Figs. 1B and 3 for profile location. D: Fine-grained and coarse-grained turbidites collected in core CAR2KS27, between 430 and 400 cm and between 517 and 500 cm below present-day seafloor, respectively. See Figs. 1 and 3 for core location. E: Core CAR2 KS26 showing bioclast-rich hyperconcentrated flow deposit and carbonate graded turbidite. For readability, cores are not figured at scale. See Figs. 1B and 4C for core location.

1000 m (sw1 in Fig. 9).

In the eastern part of Exuma Plateau, its typically wide valley abruptly entrenches the large Mesozoic drowned platform top and evolved into a narrow and deep canyon, referred to as the Exuma Canyon. Where the Exuma Valley transformed itself into a Canyon, its axis forms two successive oversized knickpoints that we will call “chutes”, through which the seafloor elevation drops abruptly 1450 m over 10 km (C1 and C2 in Fig. 9A and B). Right after the initiation of the

Exuma Canyon (ca. 9 km), a side ~4 km – wide valley drains the south part of Exuma Plateau into the Exuma Canyon (V in Figs. 1B, 6 and 9A). Another significant valley about 3 km wide called Crooked Valley (CV in Figs. 1B, 6, 9A), originating from the area between Long and Crooked Islands, referred to as Crooked Island Passage, also drains the south part of Exuma Plateau and ultimately transforms itself into a canyon (CC in Figs. 1B and 9A) which ultimately connects to the main Exuma Canyon. The transformation of Crooked Valley into a canyon is also underlined

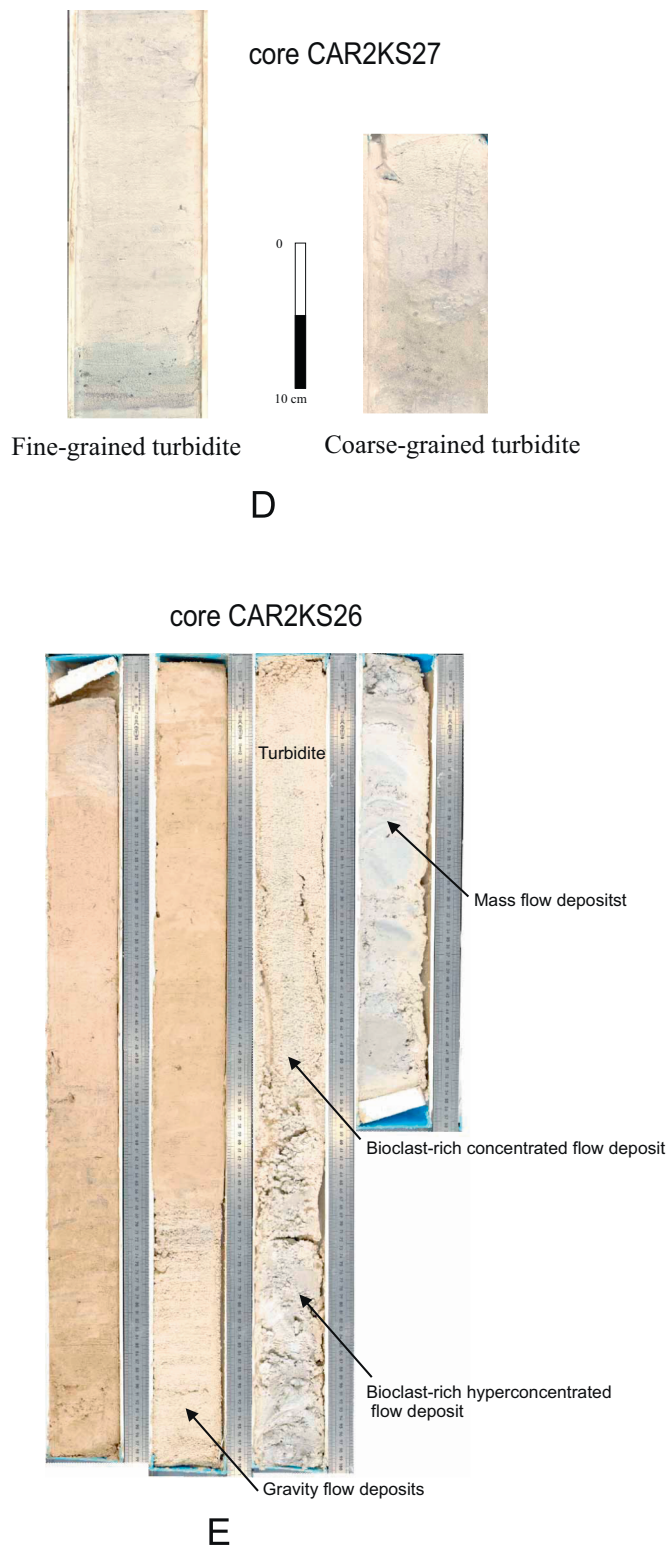


Fig. 4. (continued)

by a 400-m-high and 300-m-high chutes (C3 and C4, resp., in Fig. 9A) located 20 km away from the Bahama Escarpment following the talweg axis, and a knickpoint at its junction with Exuma Canyon K7 in Figs. 1 and 9A).

3.3. Exuma Canyon system

Within the initial canyon head area and situated directly downslope

of each main two chutes (C1 and C2), two topographic lows, expressed as two deep (300 m to 150 m, resp.), 2-km-wide depressions (Pp1 and Pp2 in Fig. 9) are juxtaposed downslope with their respective 100-m-thick topographic highs (sbd1 and sbd2 in Fig. 9) extending down-canyon. The initial major chute (C1) is 35 km upstream from the level of the Bahama escarpment following the talweg axis, where Exuma Canyon opens into the San Salvador Abyssal Plain. The 3D image of the main chute (C1) shows that the canyon axis erodes through three major steps in the overall stacked terrace typical morphology (Fig. 10). A smaller terrace is visible downslope of the chute.

Along the San Salvador slope, a roughly ovoid (lobe shape) sedimentary structure occurs that forms a 100-to-200-m-elevated topographic high (Fig. 11) at the mouth of Exuma Canyon. It is bordered in the northwest by the Bahama Escarpment and by the Samana Cay slope in the south. It extends seaward towards the San Salvador Abyssal Plain. It corresponds to the sedimentary lobe described by Ravenne et al. (1985) using the BACAR cruise results. It shows several different sized types of sedimentary structures including erosional furrows and sediment waves. The radially extended furrows are 25-km-long, 700-m-large and < 15-m-deep (f1 in Fig. 12). The proximal part of the topographic high shows at least two distinct families of asymmetric sediment waves (wavelength = 300 m, height = 10 m; sw2 in Figs. 11 and 12) with ~N130 oriented crests. The distal part of the lobed-shape levee is characterized by large tension cracks (tc in Figs. 11 and 12) extending perpendicular to the lobe radius.

The toe of the Bahama Escarpment, between 4500 and 4900 m water depth, shows numerous erosional furrows (< 5 m deep and regularly spaced with intervals around 125 m; f2 in Fig. 12) following a N-S trend. These furrows are separated from the Bahama Escarpment by a small (15 m deep and 1500 m large) depression (Fig. 13). Southward, i.e. in a down-flow direction, the furrows pass over into a field of large sediment waves (height = 20 m, wavelength = 1000-m; sw3 in Figs. 11 and 12). The crests of the sediment waves are E-W to NW-SE oriented and are roughly symmetric. At this location, a topographic relief extending parallel to the Bahama Escarpment exposes a sediment wedge echofacies located between 4500 and 4800 m water depth that documents a low amplitude stratified seismic facies (Fig. 13). In places where the sediment wedge disappear, several kilometre-large rounded, sometimes coalescing depressions extends roughly parallel to the Bahama Escarpment (Fig. 11B).

4. Discussion

The new dataset acquired in Exuma Plateau during Leg 2 of the Carambar 2 cruise allows to address four key questions: (1) How could this overall well-developed drainage system exist in such pure isolated carbonate environment, far away for any siliciclastic sediment sources? Moreover what would be the sediment volume necessary to create and maintain such a surprisingly wide valley evolving into a narrow though gigantic and deep canyon? Finally, what kind of gravity-flow processes and what would be their frequency? (2) How the drowned Cretaceous platform top and the smaller keep up banks have framed this well-organized drainage system and influenced the overall flow dynamics, the main valley morphology and its numerous tributaries, and explained the location and sudden formation of the deep canyon? (3) What is the nature of the transition between Exuma Valley and its Canyon downstream? (4) How the detailed morphology of the coarse-grained turbidite system, in addition to its surprising size and organization, be explained in a uniquely carbonate-supplied environment?

4.1. Sediment source

A first sediment source feeding Exuma Canyon could be related to direct supply from the Great Bahama Bank near Exuma Sound through tidal channels (Fig. 14). This is consistent with the analysis of turbidite components at site 632 showing large amounts of skeletal fragment and

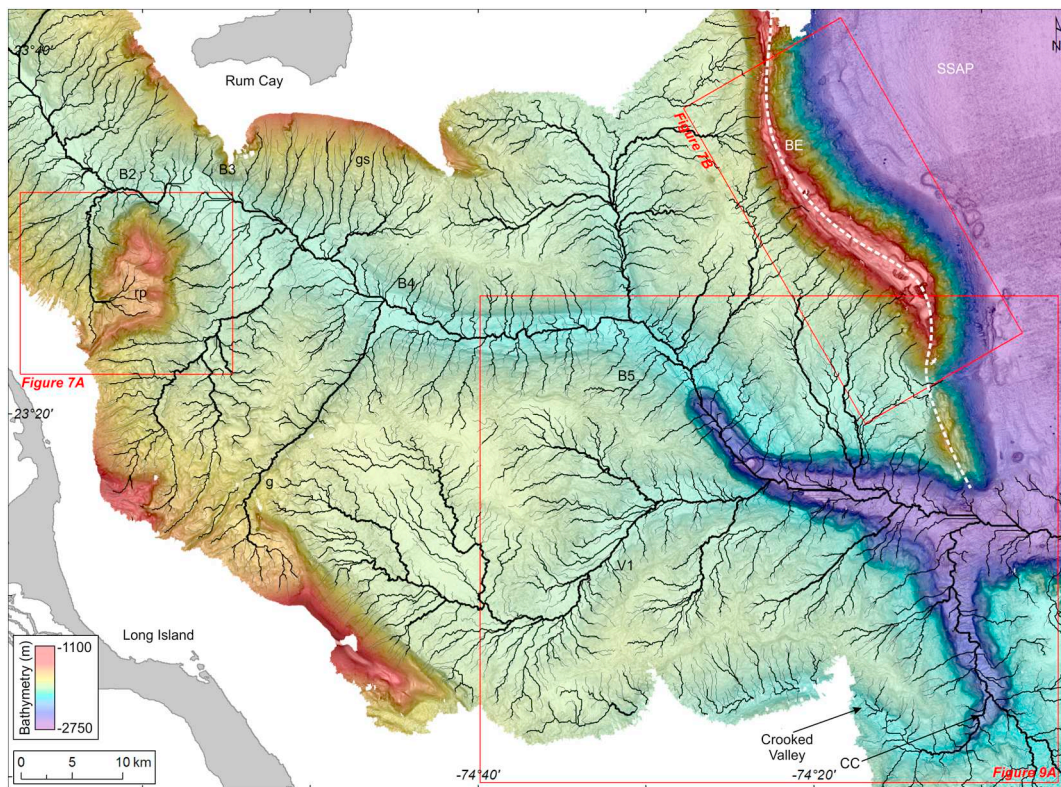


Fig. 5. Map of the drainage network on Exuma Plateau. See Fig. 1 for location and abbreviations.

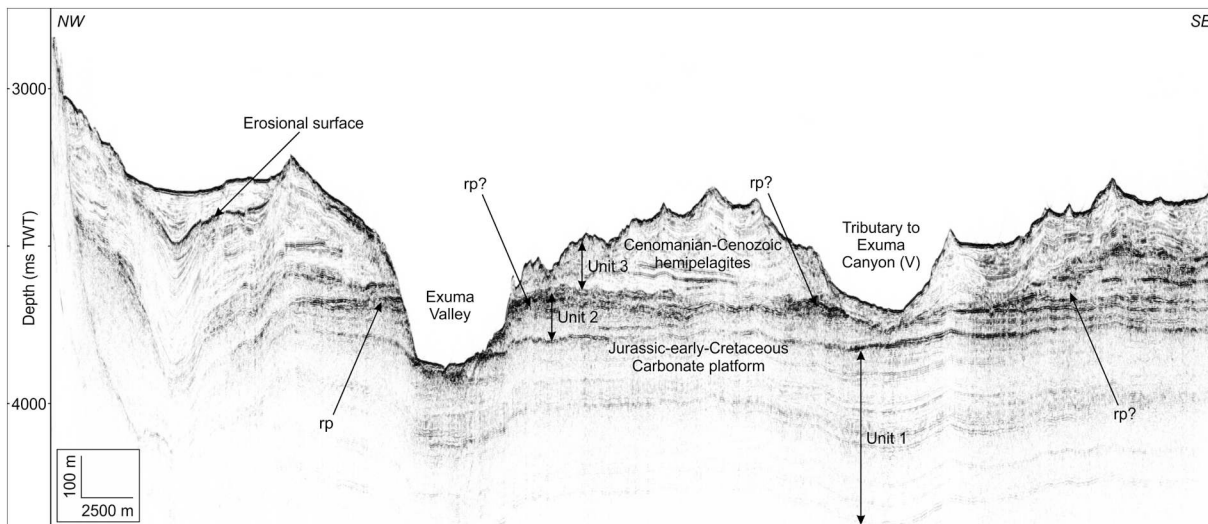


Fig. 6. High-resolution multichannel seismic cross-section through Exuma Plateau showing the Cenozoic, hemipelagic cover overlying the Mesozoic Carbonate platform entrenched by Exuma Valley and the south tributary to Exuma Canyon called Crooked Valley (CV) and Canyon (CC). Note the three seismic units described in the text. See Fig. 1B for location.

benthic organisms living on the carbonate platform (Kuhn and Meischner, 1988; Reijmer et al., 1992, 2012, 2015b). The satellite images show that the west side of Exuma Sound (Fig. 14A) and the northeast side (Schooner Cay area along west Eleuthera; Fig. 14B) are covered with large shoals identified as tidal bars (Gomes da Cruz, 2008) that are separated by channels, similar to those described by Rankey et al. (2004) and Reeder and Rankey (2008) for LBB. They correspond to the tidal bar belts of Ball (1967). According to a similar process to the one described by Mulder et al. (2017), the tidal currents could be accelerated in these tidal channels due to flow constriction and reach velocities $> 1 \text{ ms}^{-1}$ along LBB (Rankey et al., 2006) and about

1.4 ms^{-1} in Exuma Sound (Ball, 1967), particularly after the swelling of the water surface in the lagoon following the passage of hurricanes and the induced resuspension of carbonate particles produced on the lagoon. Also based on current meter measurements, Hine et al. (1981), Halley et al. (1983) and Hine (1983) suggested that the normal tidal flux was not able to transport sand off bank and that coarse grain export was due to storms. On LBB, only fine particles are expelled through the tidal channels towards the upper slope, firstly because most of the carbonate production on the platform is fine grained, and secondly because the slopes are moderate (15° on the uppermost slope, $2\text{--}4^\circ$ on the upper slope; Rankey and Doolittle, 2012; Tournadour, 2015). On

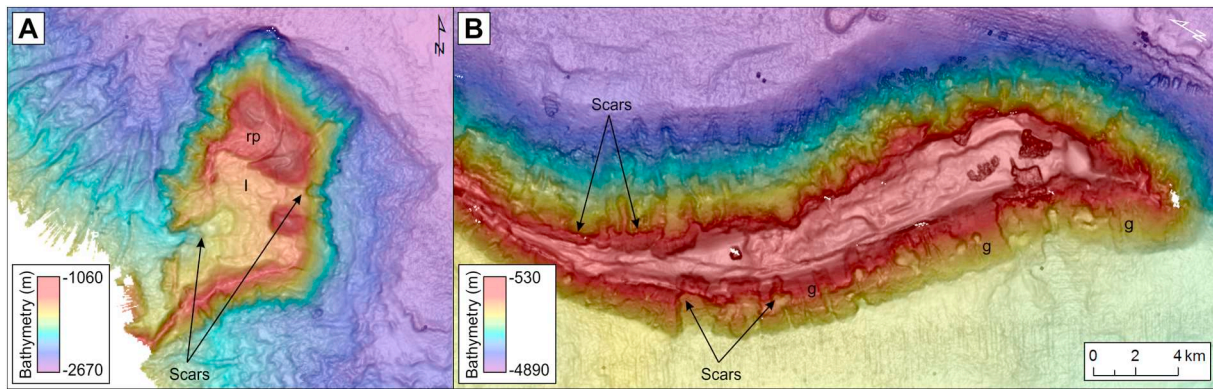


Fig. 7. Enlargements of the bathymetric map showing (A) the drowned isolated relict platform with a reef barrier (rb in Fig. 1) and the lagoon (l) and (B) the > 10 km-long drowned reef barrier bordering the Bahamas Escarpment (dep) and incised by small gullies (g). See Fig. 5 for location.

LBB, coarse-grained particles are trapped in flood and ebb tidal deltas (Reeder and Rankey, 2009a, 2009b). Conversely, along Exuma Sound, slopes can reach 45° on the upper slope and 90° on the uppermost slope (Wilber et al., 1990; Grammer et al., 1993). Therefore, coarse-grained particles (i.e. mainly bioclasts, ooids, pellets, peloids; Reijmer et al., 2012) can reach the upper slope and concentrate to form gravity flows

(Reijmer et al., 2012, 2015b). In Exuma Sound, the periplatform deposits show grain-size variations in which coarser sediments characterize interglacials marine isotope stages and finer deposits prevail during glacial stages (Rendle-Bühning and Reijmer, 2005). This pattern is opposite to the pattern observed for the westward leeward slope of GBB, which was explained to reflect the prevalence of mass transport

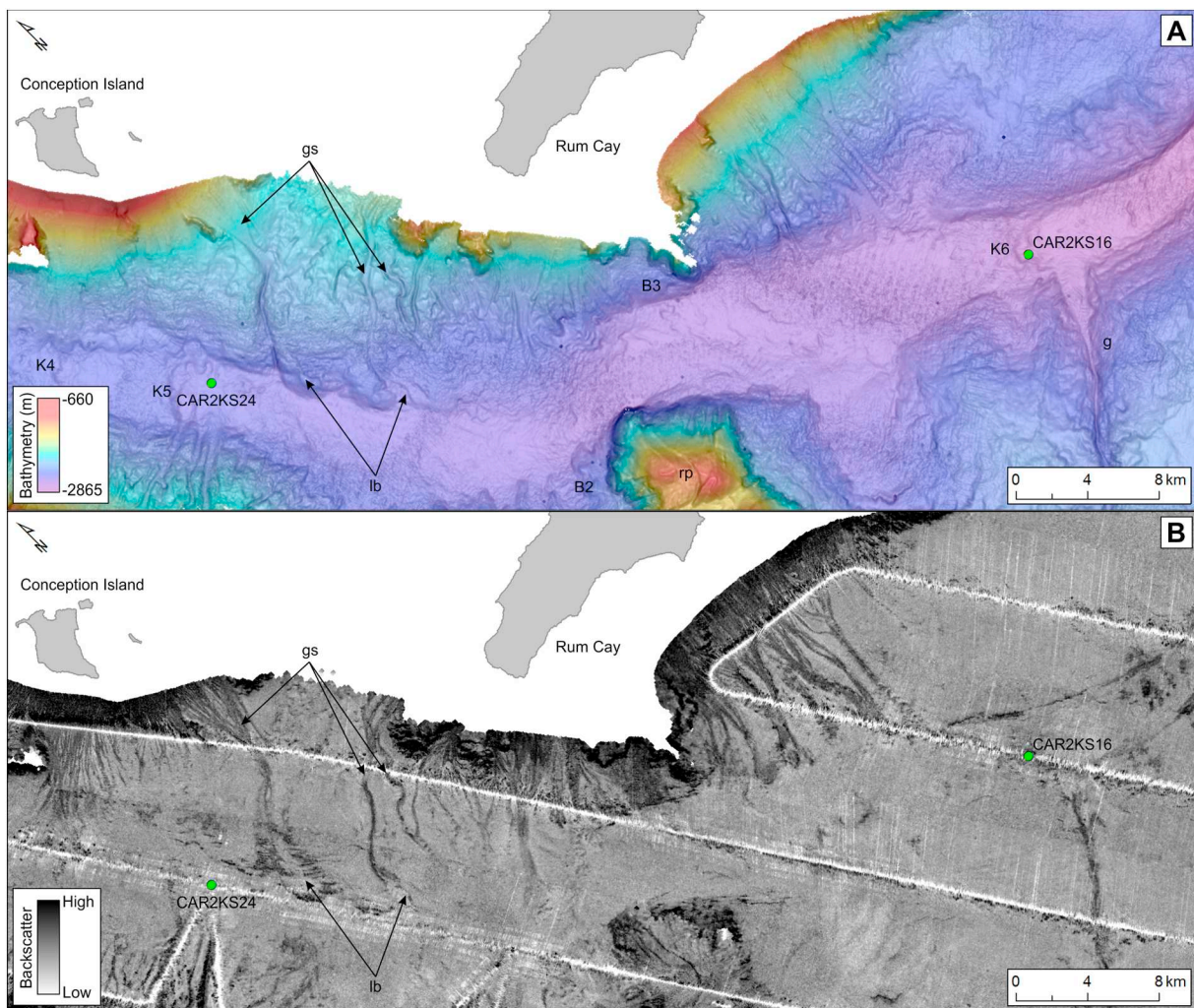


Fig. 8. Enlargement of the bathymetric map (A) and of the backscatter map (B) showing the gullied slopes (gs) and the lobate topographic bulges (lb) at the toe of Rum Cay slope. Note knickpoints (K4 to K6) located just before the northward gullied slope and the merging with the major tributary of the Exuma Valley (g) running from Long Island and the relict platform (rp) at origin of bends B2 and B3. Green dots represent core location. See Fig. 1B for location. (For interpretation of the references to color in this figure legend, the reader is referred to the web version of this article.)

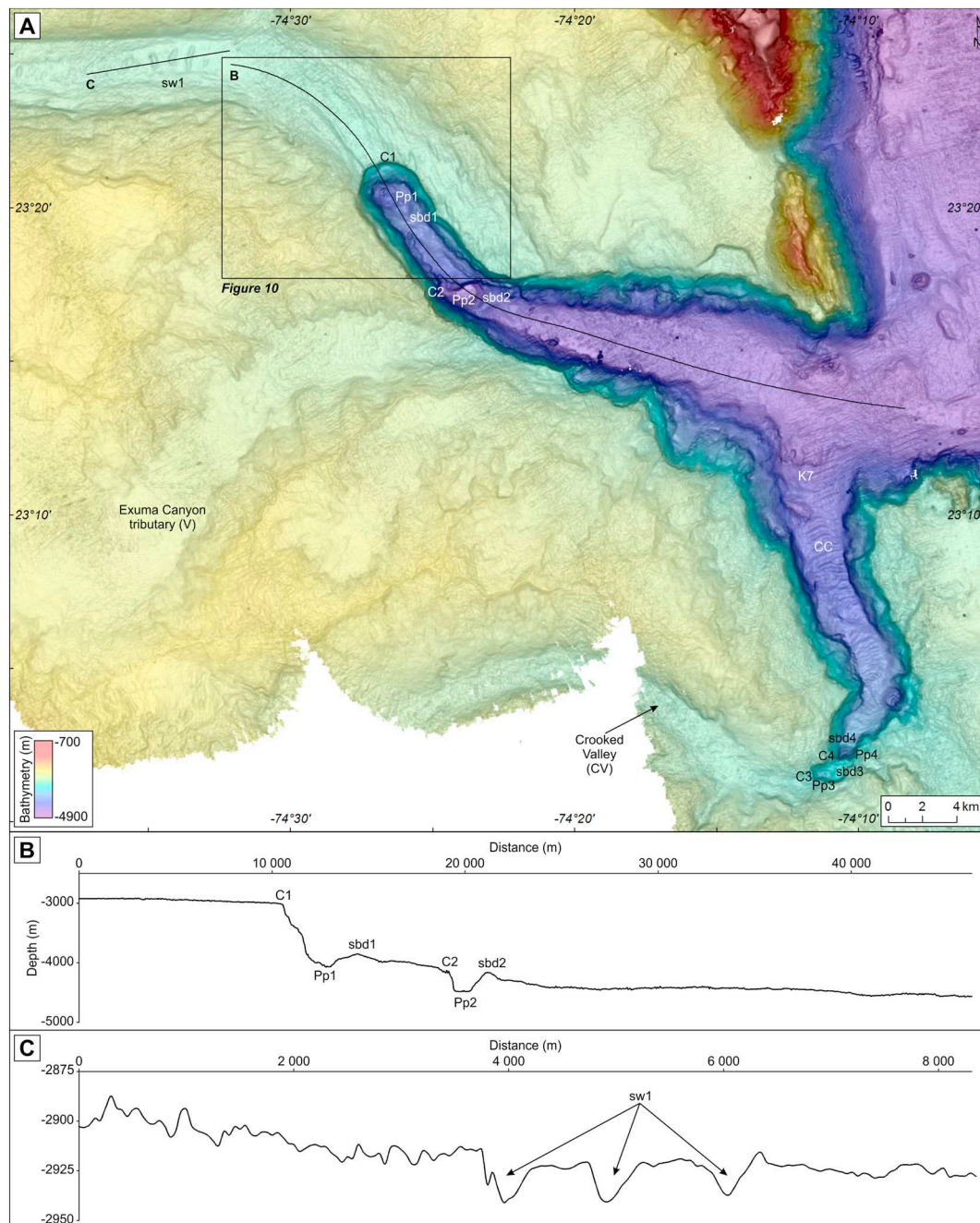


Fig. 9. Enlargement of the bathymetric map (A) in Exuma Valley (Samana Reentrant) showing the chutes (C1, C2) marking the transition between Exuma Valley and Canyon, and between the Crooked Valley (CV) and Canyon (CC; Chutes C3 and C4) the associated plunge pools (Pp1 to Pp4) and slope-break deposits (sbd1 to Sbd4) and the undulation (sw1) extending perpendicular to the slope at the end of Exuma Valley. See Fig. 5 for location. (B) Longitudinal cross-section through the giant chutes and associated plunge pools and slope-break deposits of Exuma Canyon. C: Transversal cross-section through the sediment waves.

processes (Rendle-Bühning and Reijmer, 2005). Similarly, Droxler et al. (1988) correlated the aragonite content to oxygen isotope cycles for the Plio-Pleistocene series of Exuma Sound. This correlation clearly showed the impact of platform shedding in slope sediment supply. Carbonate platforms are active during highstands (interglacials) and sedimentary material can be stored on the platform top and the adjacent upper slopes. Sediments accumulated on the upper slopes are prone to failure because of overloading and over-steepening. Mass-flow deposits thus represent a second sediment source of sediment supply from Exuma slope through mass transport (Spence and Tucker, 1997; Reijmer et al., 2012, 2015b). Mass-flow and slump deposits are described in the northwestern part of Exuma Sound by Crevello and Schlager (1980) and

Schlager and Ginsburg (1981). In addition, the area surrounding the ODP sites 631-632-633 shows intense slumping of the layered deposits lying above the Mesozoic platform (top Albian; Schlager et al., 1984; Reijmer et al., 2012, 2015b). The investigated slope area displays numerous escarpments trending perpendicular to the slope dip. They are interpreted as slump headwall scarps and are essentially shallow-rooted failures (failure surface < 120 m; Fabregas, 2018; Fig. 1C). However, the ODP data suggest that the entire area might be subjected to deeply-rooted faults leading to large-scale slumps propagating basinward (Austin et al., 1996, 1988). The slopes surrounding Exuma Sound reach 40° on the upper slope with locally a vertical uppermost slope similar to the slopes of the Tongue of the Ocean (Grammer et al., 1993). These

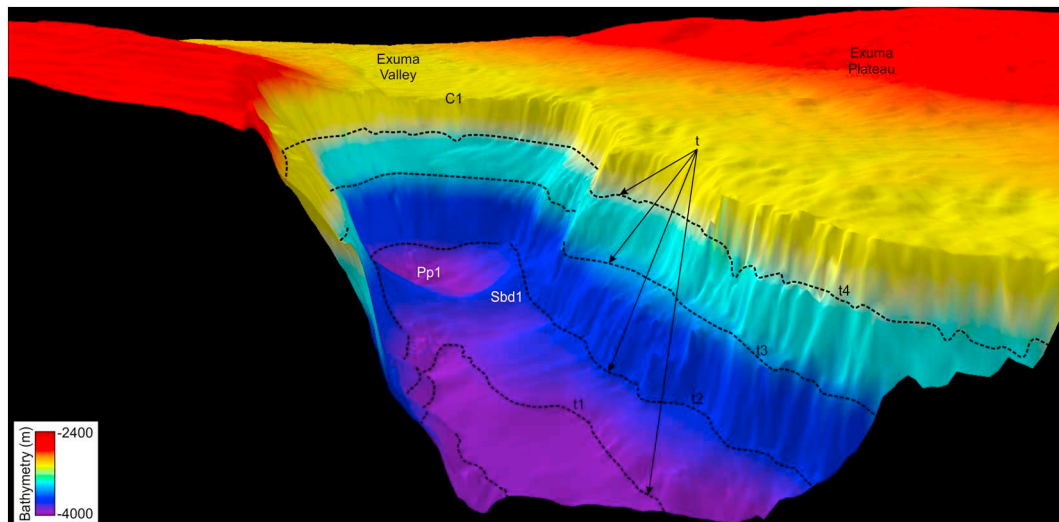


Fig. 10. 3D view showing the superposed terraces (t1 to t4) and chute C1, Plunge pool Pp1 and Slope-break deposit Sbd1 marking the transition between Exuma Valley and Exuma Canyon. See Fig. 9A for location.

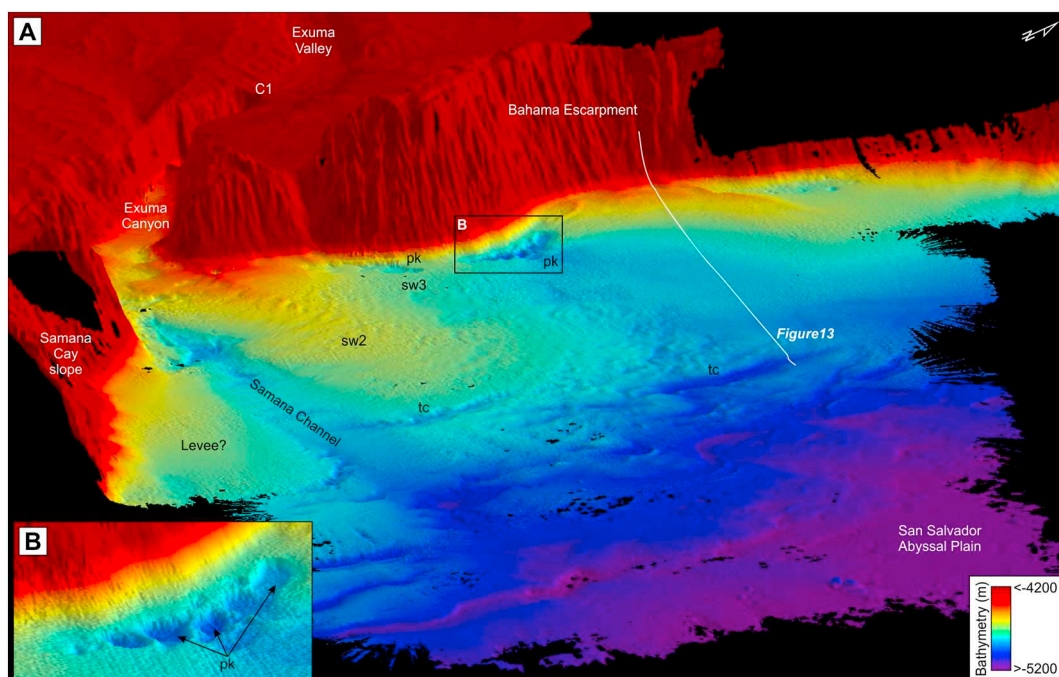


Fig. 11. (A) 3D view of the San Salvador carbonate turbidite system developed at the mouth of Exuma Canyon. It extends in the San Salvador Abyssal Plain and is bordered by Samana Cay slope and Bahama Escarpment. pk: pockmarks; sw2 and sw3: sediment waves; tc: tension cracks. (B) Enlargement of the bathymetric map showing alignment of coalescing pockmarks.

steep slopes likely represent the most influential pre-conditioning factor for slumping (Spence and Tucker, 1997).

On leeward slopes (Great Bahama Bank) or in areas not affected by energetic contour currents such as Exuma Sound, mass flow deposits including debrites are frequently encountered. Instabilities triggered directly during highstands, when carbonate particles form and accumulate on the slope, such as the mass flow deposits described by Crevello and Schlager (1980), or occurring during a lowering of the sea-level resulting in excess pore pressure accumulating below cemented levels (Spence and Tucker, 1997; Jo et al., 2015; Reijmer et al., 2015b; Wunsch et al., 2016, 2018) such as on Great Bahama Bank. Finally, mass-flow deposits in Exuma Canyon occur interbedded with fine-grained glacial peri-platform ooze (Kuhn and Meischner, 1988; Reijmer et al., 1988, 2012, 2015b).

The presence of numerous gullies confirms that intense erosion occurs along the steep slopes of Exuma suggesting active sediment transfer from the upper slope into Exuma Valley. Downslope, the basin exhibits gullied edges forming small turbidite lobes (Crevello and Schlager, 1980). In addition, the presence of steep slopes and related erosion around Exuma Sound would explain the large amount of planktonic foraminifers (the large abundance of planktonic foraminifers is related to failures of the slopes on which the pelagic ooze had initially accumulated) and little amount of detritus produced on the platform within the turbidites at Site 628. Several lines of evidences suggest that turbidity currents are supplied either by particle exported by tidal flush (Mulder et al., 2017) which do not explain the transport of planktonic foraminifers because they are not accumulated on the bank top, or by transformation of mass-failures.

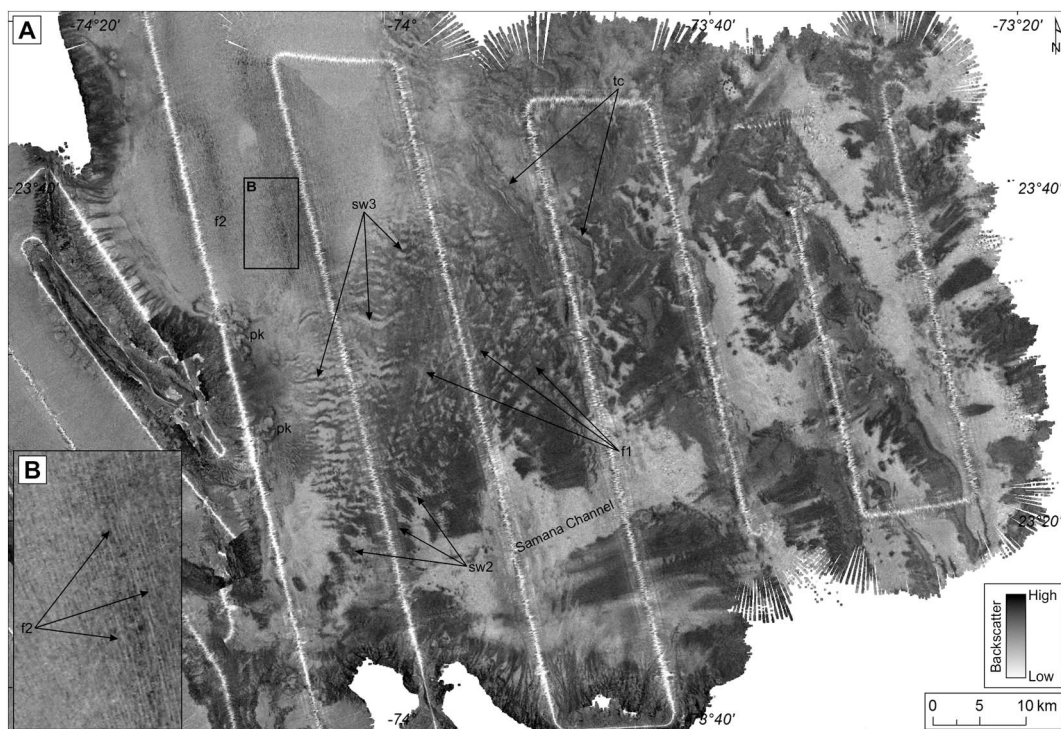


Fig. 12. Enlargement of the backscatter image of the San Salvador turbidite system. Low reflectivity corresponds to light tones; high reflectivity corresponds to dark tones. f1, f2: furrows; pk: pockmarks; sw2 and sw3: sediment waves; tc: tension cracks. B: Enlargement of the map showing furrows f2. See Fig. 1B for location.

The high-amplitude echofacies observed in the axis of Exuma Valley at the mouth of Exuma Sound (Fig. 4C) correspond to the presence of gravity-flow deposits. Core CAR2KS26 shows a long sequence that is coarse (bioclast-rich) and ungraded at its base and becomes progressively graded (Fig. 4E). It is interpreted as the stack of mass-flow deposits and hyperconcentrated to concentrated flow deposits (poorly-graded Ta Bouma facies) passing progressively to a graded carbonate turbidite. In this core, mass-flow deposits represent more than the half of core length. The deposits form the “moustache shape structures” with layered echofacies and strong contrast in acoustic impedance contrast observed at the southeastern exit of Exuma both suggest deposition of levee deposits made by staked turbidite resulting from the spilling of turbidity currents at this location. There, the main valley axis makes a curve to the right that could explain some spill-over of gravity flow towards the left bank (Fig. 4A). The graded coarse-grained or fine-grained sequence observed in core CAR2KS27 are interpreted as classical carbonate Bouma sequences (Fig. 4D). This agrees with the

observation by Crevello and Schlager (1980) who demonstrated that turbidity currents could differentiate along Exuma Sound slope and basin and reach as far as its southeastern basin extremity. Reijmer et al. (2012, 2015b) linked the composition variations of calciturbidites and calcidebrites to sea level fluctuations alternating flooding and exposure of the carbonate platform top, in particular explaining highstand calciturbidite occurrence and their conspicuous absence during lowstands (Droxler and Schlager, 1985). Moreover sea level falls and rises along the basin high angle upper slope are expected to destabilize the upper platform edge and trigger calcidebrites (Grammer et al., 1993). Core CAR2KS24 collected in Exuma Valley contains series of calciturbidites indicating sediment transport by gravity flows reaching as far as that particular location (Fig. 15A).

The supply from the sides of Exuma Valley including flanks of island bordering the valley and main valley tributaries also appears to represent a substantial source of sediment. This feature has already been underlined by Mulder et al. (2018) for the Great Abaco Canyon and

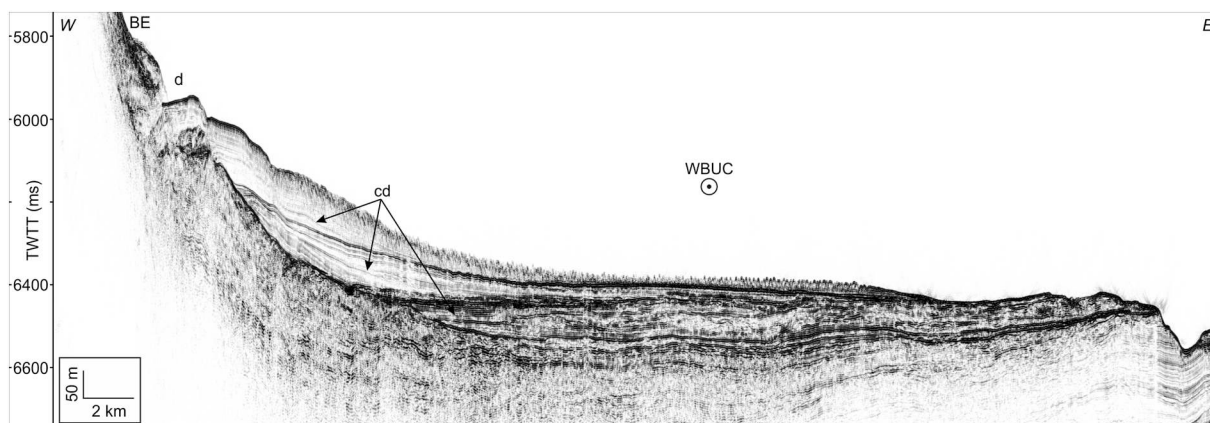


Fig. 13. Multichannel W-E seismic profile crossing the contourite system related to the Western Boundary Undercurrent (WBUC) and the San Salvador turbidite system along the Bahama Escarpment (BE). d: depression (moat); cd: contourite drift. WBUC: Western Boundary Undercurrent. See Figs. 1B and 11 for location.

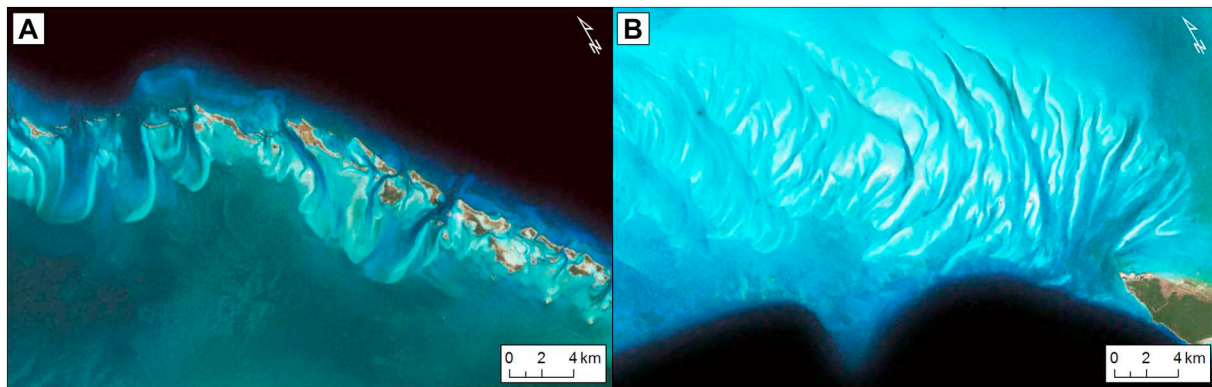


Fig. 14. Satellite Images showing the tidal channels and related bars, north of Exuma Sound (World Imagery Sources: Esri, DigitalGlobe, GeoEye, i-cubed, USDA FSA, USGS, AEX, Getmapping, Aerogrid, IGN, IGP, swisstopo, and the GIS User Community). See Fig. 1A for location.

seems to be a common feature of these large deep-water carbonate canyons. Numerous gullies dissect the Rum Cay or Conception Island slopes before merging with the canyon (gs in Fig. 8). The image of the drainage system as shown in Fig. 8 is consistent with this interpretation. Some of the gullies directly connect with the main Exuma Valley suggesting that no or little deposition occurs before they merge with the main valley. Conversely, other gullies are connected to a lobate bulge suggesting that some flows lacked enough inertia to reach the valley itself. In this case, bulges would correspond to an accumulation of mass-flow deposits or possibly to freezing of a single slide deposit (lb in Fig. 8). The abundance of bulges suggests that this kind of sediment supply is frequently encountered along the steep slope bordering Exuma Plateau. The presence of knickpoints located just at the junction of gullies (K3, K4, K5) or of major tributaries (K6) suggest a more intense sedimentary activity in these tributaries than in the main Exuma Valley. Direct supply from the uppermost slope of Rum Cay is evidenced by the lithology observed at the bottom of core CAR2KS16 collected in Exuma Valley just south of Rum Cay (Fig. 15B). The core shows a 65-cm-thick sequence with a graded coarse-grained calcirudite dominated by coral fragments, which is interpreted as a hyperconcentrated to concentrated flow deposit. This kind of flow needs steep slopes to move and motion usually occurs along a short runoff distance (Mulder and Alexander, 2001) suggesting that the flow was initiated just at the toe of the reef barrier at the platform margin near Rum Cay. As these grain-supported flows need steep slopes to keep moving, the Rum Cay barrier seems the most probable source. The longest gully connecting to Exuma Valley is 30 km long and initiates directly from the slope of Long Island. The presence of a 50-m-high knickpoint just upslope the gully connection with the valley (K6 in Fig. 8A) suggests an important flow activity in this gully when compared to the main Exuma Valley. The “moustache shape structures” (Fig. 4B) exhibiting layered echofacies can be interpreted as levees and strongly suggest the presence of differentiated turbidity currents at this location, consistently with results of Crevello and Schlager (1980). The smaller gullies running along Rum Cay and Conception Island also form knickpoints just upstream of the point where they merge with the main Exuma Valley, suggesting recent sediment flow activity and flows with a higher energy than those flowing in the main Exuma Channel (K4 and K5 in Fig. 8A). The presence of undulations on the floor of the main Exuma Valley could correspond either to coarse-grained sediment waves or to erosional steps (sw1 in Fig. 9A and Fig. 9C). It confirms active sediment flow processes along the valley floor. Nevertheless, our data are not accurate enough to characterize the origin of these undulations and to precise the erosional or depositional nature of the flow.

4.2. Exuma Plateau and relict platforms

Because of its relatively flat topography, the area connecting the

exit of Exuma Sound to the abyssal plain at the level of the Bahama Escarpment is referred to Exuma Plateau. Its flat topography is rooted in the underlying Jurassic–early Cretaceous carbonate flat top platform that mostly drowned during late Albian (Schlager et al., 1984). The platform is imaged on the multichannel seismic grid by sub-parallel and sub-horizontal stacked reflectors and its interpreted partial drowning top is marked by a couple of stronger high amplitude reflectors (Fig. 6). The Jurassic–early Cretaceous platform top in Exuma Plateau was not completely drowned in the late Albian; in several instances, small parts of the platform continued to grow forming isolated keep-up banks that ultimately drowned. Some of them are clearly exposed in the water column while others are buried as the main platform top by a Cenomanian to Cenozoic periplatform 300–400-m-thick cover (rp in Fig. 6) characterized by lower velocity of 1700 ms^{-1} than the underlying Jurassic–Lower Cretaceous platform (Schlager et al., 1984; Fig. 6). The two most conspicuous keep-up banks are an isolated topographic high, rising some 1100 m above the seafloor between Long Island and Rum Cay (rp in Figs. 1 and 7A) and the elongated positive topography along the edge of the modern Bahama Escarpment, interpreted as a relict narrow keep up bank of probable Cenomanian age (Figs. 1 and 7B). The former is also interpreted as a relict late Cretaceous (post Albian) isolated carbonate bank characterized by an irregular top displaying systematic higher reliefs on its eastern edge, interpreted as an ultimate barrier reef and on its northern part as a back-stepped, staircase morphology, both typical of the ultimate growth phase of the keep-up bank on its windward high energy side (assuming that modern easterly/north-easterly wind preferential directions were unchanged in the late Cretaceous), while the lower topography on its center and western margin can be explained by preferential early drowning on the low energy leeside of the bank. The elongated keep-up relict bank, lining the eastern part of the Exuma Plateau and enhancing the Bahama Escarpment extreme high relief, would correspond to the latest growth activity of the Cretaceous platform in the Exuma Plateau along its ocean-facing position eastern edge (dep in Figs. 1 and 7B). In that particular area, the carbonate growth conditions were more favorable, explaining the formation of the conspicuous high relief elongated narrow keep-up bank terminated by a Cenomanian drowning event (Fig. 7B). The steep slopes of both most developed keep-up banks platforms on Exuma Plateau are intensely eroded as suggested by numerous scallops, slump scars, and gullies incising their margins (Figs. 1B, 7A and g in Fig. 7B). Long Island and Rum Cay are two banks that have kept growing since the late Cretaceous, although their northern extremities (B2 in Figs. 1 and 5) correspond to partially drowned areas of Long Island and Rum Cay keep-up banks, at about the same time as the other two isolated drowned keep-up banks described earlier (Fig. 7). The orientation of the valley seems to be constrained by the drowned topography of the Cretaceous platform. In particular, bends are localised at locations where the valley axis is perturbed by the

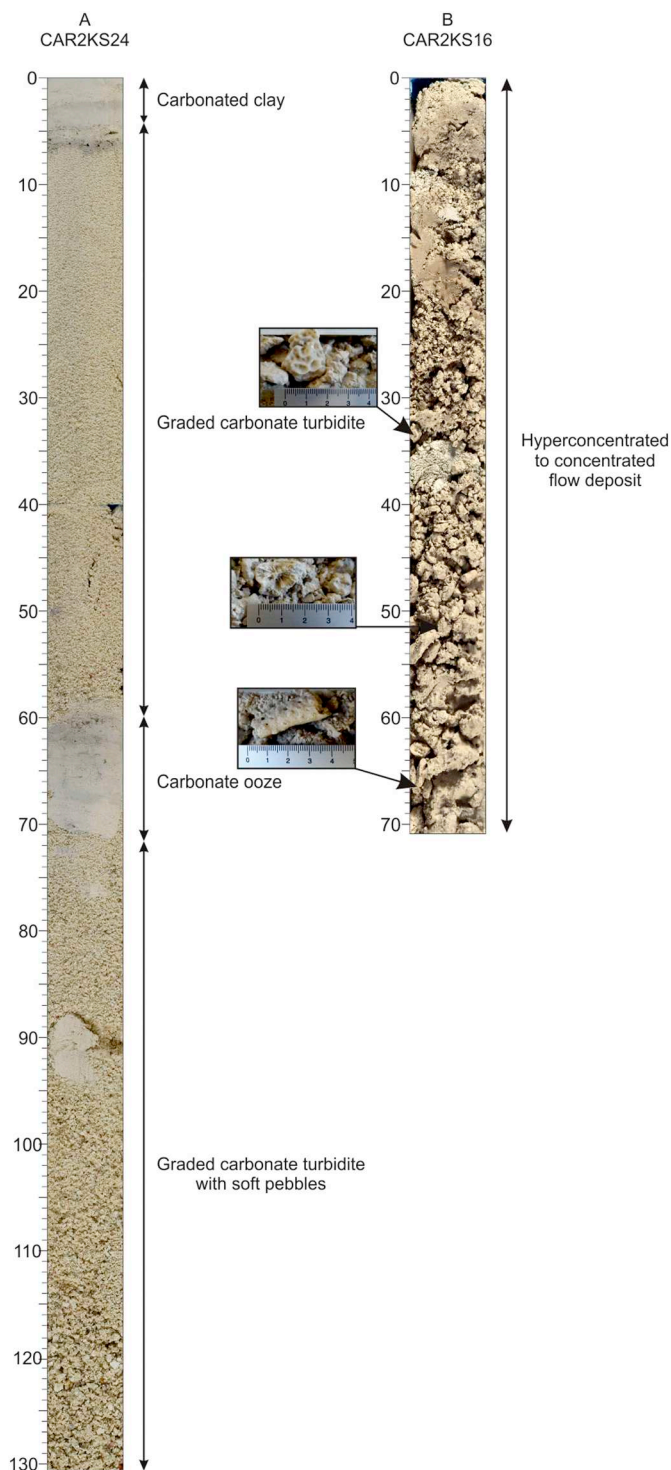


Fig. 15. (A) Photograph of core CAR2KS24 (455 to 587 cm) located in Exuma Valley showing two stacked carbonated turbidites. (B) Photograph of core CAR2KS16 (300 to 380 cm below present-day seafloor) showing a graded calcirudite interpreted as a hyperconcentrated to concentrated flow deposit initiated at the toe of the Rum Cay platform edge. Insets show enlargements of coral fragment extracted from core CAR2KS16. See Figs. 1B and 4B for location.

relict platforms (B1 and B2/B3 in Figs. 1 and 5).

In the eastern part of Exuma Plateau, Exuma Valley incises the entire Cenomanian-Cenozoic cover and runs on the high amplitude reflectors corresponding to the top the Mesozoic carbonate platform (Fig. 6). This observation would suggest that the deep canyon incision further down the valley, connecting Exuma Plateau with the North

Atlantic abyssal plain, was not initiated before the complete drowning of the platform top; otherwise, wall aggradation would have led to the incision of a larger part of Jurassic-Lower Cretaceous deposits. The newly acquired seismic data sets do not show any evidence of structural control for the canyon occurrence and its orientation. However, the overall canyon orientation in Exuma Plateau mimics the one of Great Abaco Canyon which is clearly structurally controlled by large transform faults (Great Abaco Fracture Zone; Mullins et al., 1982). The Exuma Canyon orientation also parallels the edge of Mayaguana Island that possibly relates to a fault direction (Kindler et al., 2011). Another hypothesis would be that the canyon is in fact formed simultaneously to large reentrants such as the one observed at the mouth of Tongue Of The Ocean, Northeast Providence Channel, or Eleuthera Valley. In that case the age of the canyon could be older than Upper Cretaceous and, therefore, its formation be contemporaneous to the Samana Reentrant located southeastward and Lower Cretaceous in age (Fig. 1B; Corso, 1983). On the other hand, present-day western current strength (WBUC or deeper Antarctic water masses) along the Bahama Escarpment is too weak to explain the size of the incision. These currents were not present in most of the Mesozoic since the thermohaline conveyor belt was not active (Thomas and Via, 2007).

4.3. Exuma Valley-Canyon transition

Associated chutes and depressions occur at the location where the large Exuma Valley very suddenly transforms itself into the deep and narrow Exuma Canyon (Fig. 9). In Exuma and Crooked valleys all of the deepest rounded depressions are located down of major chutes. Soulet et al. (2016) showed for the Polcevera Canyon in the Ligurian Margin and Mitchell (2006) in Southeast Australia that large knickpoints could be related to faults running perpendicularly to the channel axes. However, no evidence of faults running parallel to the chute is observed at the location of the chutes in our study area. In the case of the Great Abaco Canyon, (north of the Exuma Plateau) the only fault observed is oriented parallel to the canyon (Sheridan et al., 1981, 1988) i.e. perpendicular to the chutes. In addition, no deep-rooted structures such as fluid escape structures seem to occur below these depressions. The only fluid escape structures observed in the study area are pockmarks (pk in Fig. 11) aligned at the toe of slope of the Bahama Escarpment and are related to the bench located at the toe of this large escarpment (Schlager et al., 1984). We cannot completely exclude in this study the hypothesis that the initial genesis of the topographic depressions observed at the base of the chutes could be related to sub-bottom fluids, either related to the presence of Jurassic salt and gas hydrates or to brine seeps as observed in other areas such as the basis of the Campeche Scarp (Paull and Neumann, 1987). However currently, each depression corresponds to a plunge pool formed by enhanced erosion related to flow expansion and increased turbulence during a hydraulic jump generated by either long-duration and/or frequent turbulent sediment-laden flows (Komar, 1971). The topographic high located just downdip of the pool would thus correspond to slope-break deposits (Mulder and Alexander, 2001).

The size of the chutes and of their associated plunge pools in addition to the observations that the pools are not filled and buried “paleo-plunge-pool” do not exist would strongly suggest that these morphological depressions stayed geographically at the same location for a very long time and that activity of sediment-laden flows in Exuma Valley and Canyon have remained intense, frequent, and continuous. The first major plunge pool is not located along the N-S oriented Bahama Escarpment but approx. 35 km westward (Fig. 1). This suggests that the canyon formed by regressive erosion in this area. However, the lack of a paleo-plunge pool suggests that regressive erosion probably occurred during the initiation of the canyon system. This occurred most likely shortly after the general regressive erosion of the whole platform. This retreat is estimated to range from 5 km (Freeman-Lynde et al., 1981; Land et al., 1999) to 15 km (Paull and Dillon, 1980) using

carbonate facies analogy between Exuma platform and buried platform with a similar age in the Gulf of Mexico. In the Samana Reentrant, regressive erosion might have been increased because of the early Cretaceous deep water chalks are much easier to erode than highly cemented shallow water carbonate limestone of the rest of the Jurassic – early Cretaceous platform.

The depth range and style of the three superposed staircase like along the walls of Exuma Canyon display great similarities to the three stacked terraces observed at the location of the first chute (C1 in Fig. 1) and the fourth one located downslope could correspond to mechanically-resistant stratigraphic levels in a Mesozoic carbonate platform succession (Schlager et al., 1984; Fig. 10). This suggests that the location of the chutes and plunge pools possibly is related to a change in rock lithology at the present-day edge of the Cretaceous carbonate platform. This is also consistent with the flatness of the valley between the individual chutes. Using the analogy with the Great Abaco Canyon stratigraphic section, the superposed steps could then correspond to the boundary between limestones (Tithonian) and chalk (Upper Jurassic/Lower Cretaceous) for the deepest one, the boundary between chalk and the Aptian clay for the second one and to the top of the carbonate platform deposit (Cenomanian) for the last one (Benson and Sheridan, 1978; Mullins et al., 1982). Downslope of the chutes, the canyons remains relatively flat suggesting once again that the channel most likely follows a stratigraphic level of the ancient Mesozoic platform. Considering flow hydrodynamics, a given mass-flow traveling down the Exuma Valley and Canyon encounters successive chutes, each generating a hydraulic jump and increasing flow turbulence. Similar mechanisms have been described at the mouth of siliciclastic channels in sandy turbidite systems but at a lower scale (Channel-Lobe Transition Zone, CLTZ; Wynn et al., 2002). At this CLTZ the hydraulic jump is at origin of the formation of erosional features. Just downslope of the chute, flow velocity decreases and the flow height increases as the flow passes from a supercritical to a subcritical state (Komar, 1971). These successive flow transformations increase subsequently both flow capacity and competency, thus enhancing flow dilution. Just after the area of increased turbulence, flow becomes more stable and particles that have just been eroded in the pool can settle, thus forming the slope-break deposits (sbd1 and sbd2 in Fig. 9).

4.4. The coarse-grained turbidite system

When crossing the Bahama Escarpment, the canyon becomes unconfined in the San Salvador Abyssal Plain and evolves into a channel (Samana Channel in Figs. 1, 11 and 12). The previously confined flows in the deep and narrow canyon experience another hydraulic jump due to both channel enlargement and axis slope reduction (Figs. 1, 11 and 12). The rapid flow deceleration induces flow transition to a subcritical state (Migeon et al., 2001). As a result, the flows thicken, allowing spilling over and the build-up of a large lobe-shaped sedimentary levee (SL in Fig. 1B). The location of this levee on the left flank of the channel could appear unusual, because the Coriolis force deflection, though small in the tropical regions, is expected to be to the right of the flow. The Samana Channel itself is following the toe of Samana Cay steep slope, confining any flow and preventing spilling and levee construction on its right flank. This suggests that most of the flows (i.e., the part prevented from spilling) continues downslope the channel. The radial furrows (f1 in Fig. 12A) are consistent with frequent overbanking of the whole flow (rather than the spilling of their upper part). In addition, the presence of furrows indicates that the flows passing through the Bahama Escarpment are flows with a high momentum. BACAR cores (Cartwright, 1985) showed that most of the mass-flow deposits consist of ungraded to roughly graded carbonate sands and gravels (Fig. 2) suggesting that part of the flows entering abyssal plain at the mouth of the Exuma Canyon are coarse-grained concentrated flows. Consequently, the levee complex is frequently bathed with high-energy-coarse-grained inertia flows with a high-erosive potential. The

asymmetric sediment waves observed in the proximal part of the levee (sw2 in Figs. 11A and 12A) evidence a crest orientation that is consistent with flow spilling over a channel flank (Migeon et al., 2001). The superimposition of sediment waves over the furrows suggests a decrease in energy of the spilling flows, related either to a decrease in mass flow supply (alloycyclic process) or to the progressive increase of the levee height (autocyclic process). The sedimentary levee along the left flank of the channel forms the most prominent feature of the deep-sea fan, at the mouth of Exuma Canyon. It significantly decreases in height with distance suggesting that most of the sediment supply consists of coarse particles and that only a minor part is transported further downslope. Analysis of core particles (Cartwright, 1985; Schmitt, 2013) observed clasts whose nature reveals that a substantial part of the material derived from the platform and upper slope environments, consistent with a transport by sustained mass flows. However, the presence of siliceous fragments (flintstone; Fig. 2C) suggests that also a substantial supply originates from the Bahama Escarpment itself. The mostly neritic bioclastic coarse-grained distinct layers in cores from the levee complex (Cartwright, 1985) have to be supplied through the Exuma Canyon by high-energy, long-runout inertia flow and their origin in the upper slopes surrounding the Exuma shallow water carbonate platform. These bioclastic turbidite layers interfinger with lithoclastic fragment and rock-avalanche accumulation generated by short runout mass transport processes through the regressive Bahama Escarpment erosion (Freeman-Lynde and Ryan, 1981; Fig. 2C). These later accumulation, rich in lithoclastic fragments are only observed in close proximity of the toe of the Bahama Escarpment and do not occur in the mid and distal parts of the fan (Cartwright, 1985). Moreover large cracks are observed on the levee (tc in Figs. 11A and 12A). Because they are tangential to the lobe radius, it is logical to suggest that they form in response to gravitational spreading of the whole sedimentary pile, referred to tensional cracks. This spreading corresponds to creeping with a low-deformation rate of the soft sediment progressively piling up above the rigid oceanic crust basement. It is a similar process as the one observed by Harwood and Towers (1988) for the LBB slope but in this study, creeping involves the entire sedimentary pile. The location and orientation of the tensional cracks may be inherited by fault structural direction in the oceanic crust, because the sediment cover is relatively thin; the maximum thickness of the gravity flow accumulation was estimated to about 1 km based on seismic (Ravenne, 2002).

The coarse-grained turbidite system at the mouth of Exuma Canyon accumulating at the toe of the Bahama Escarpment forms a complete submarine fan with a run-out > 120 km. Most of the deposits found in the distal part of the system are coarse grained (Cartwright, 1985) which drastically differs from model of high runout “fine grained, large size Carbonate Submarine Fan” (CSF of Payros and Pujalte, 2008). In their CSF model, these authors state that “large-scale erosive canyons seem to be rare as major slope feeder systems and that some of the features interpreted as slope canyons could actually be upper slope gullies” (Payros and Pujalte, 2008). These authors also note that Pleistocene CSFs located in offshore South Australia are supplied by ancient large canyon inherited from Pleistocene lowstand times and “that their formation was not directly related to the processes leading to CSF”. The high gradients of the thick long-lived Bahama Platform margins, from upper slope down to abyssal depths exceeding 4500 m, was favorable for large and deep canyon development for the efficient transfers of neritic carbonate sediments from the platform edge to the abyssal plain. These high bathymetric gradient generated very high flow dynamics in the Exuma Canyon that allow transport of coarse particles down to the most distal part of the sediment dispersal system. However, the presence of gigantic canyons seems related to the presence of the Bahama Escarpment that probably the represents the “special circumstances” suggested by Payros and Pujalte (2008) to explain the presence of canyons in deep-sea carbonate environments and including also structural direction in the oceanic crust.

Furrows with a N-S direction extending approximately parallel to the Bahama Escarpment (f2 in Fig. 12), oriented parallel to the WBUC flow, are interpreted to be formed by seafloor erosion due to the contour current flow strength and, therefore, would attest of the very-high current energy at the toe of the Bahama Escarpment (Stow et al., 2009). Consequently, the small depressions located between furrows and the Bahama Escarpment would correspond to a moat; the topographic high located southward of the moat can be interpreted as a contourite drift with its classical “muscle” shape revealing combined onlap and downlap geometries (Fig. 13). The contourite drift is associated sediment wave field characterized by a long wavelength (sw3 in Figs. 11A and 12A) suggesting that the contour current became depositional at this location. This decrease in energy is consistent with the formation of an eastward and southward prograding detached drift at about a water depth of 4450 m. The drift accumulation is still separated from the Bahama Escarpment by a well-developed moat, becoming deeper while the drift accumulation is growing. Cores retrieved from this particular drift deposit (point out to fine-grained clay rich accumulation), typical of contourite lithology (Droxler, 1984). The high accumulation rates of those siliciclastic contourites buried rapidly the neritic carbonate mass-flow deposits, preventing their total dissolution at water depths undersaturated with respect to aragonite and magnesian calcite, typical mineralogy of neritic carbonates (Droxler et al., 1991).

Rounded, 0.75–1.5 km-in diameter and 100–150 m-in depth isolated or coalescing pockmarks (pk in Fig. 11) clearly occur within the moat on the toe of the BE. The presence of fluid escape structures at this location are interpreted to have originated through the combined presence of Jurassic salt and gas hydrates in the underlying sediment cover or to brine seeps (Paul and Neumann, 1987).

5. Conclusions

The recent bathymetric and multichannel high-resolution seismic surveys of Exuma Plateau image in exquisite details a wide Exuma Valley abruptly transitioning into a deep narrow canyon and reveal an unusual large-sized carbonate talweg system, particularly when considering the depth of the incision and the coarse-grained nature of the abyssal plain deposits at the mouth of the system. Initially a quite shallow wide valley alimented by numerous well-organized gullies is observed, similar to those incising the continental shelf in siliciclastic systems, though extending parallel to the margin. Turbidity currents and other type of mass flows along the valley channel transported particles originating either directly from the carbonate platform tops, or from the erosion of the steep upper slopes surrounding Exuma Plateau. The Exuma valley does not incise deep in the Jurassic-Lower Cretaceous carbonate platform, though when the valley abruptly transition into a canyon, a large part of the platform is deeply incised suggesting that the initiation of the canyon incision by regressive erosion was probably not older than the mid Cretaceous drowning of the Mesozoic platform top.

Successive gigantic chutes at the wide valley/deep canyon abrupt transition are rather unique and spectacular by their unusually large overall dimensions. Two of those chutes, with a topographic drop of 1450 m at the valley/canyon transition, bring the canyon floor at depths close to adjacent abyssal plain. The system, though at bathyal depths, morphologically resembles subaerial outsized waterfalls and channels which have to be formed with very high-energy submarine flows that build a coarse-grained turbidite system at its exit. Obviously, the major difference with a subaerial waterfall, alimented by a continuous river flow, that the Exuma Plateau drainage system was carved by numerous, though non-permanent, gravity flows. Large-scale observed morphological structures, such as giant plunge-pools, emphasize the tremendous erosive power of the sediment-laden flows and the hydraulic jump, high erosive impacts occurring at the level of these chutes. The turbidite deep-sea fan system, developed in the San Salvador Abyssal Plain at the mouth of this enormous Exuma Canyon subaquatic well-organized drainage system, contrasts by its relatively

small size, < 100-km in length, although the fan system shows evidence of overflow by concentrated flow containing coarse-grained sediments. Moreover, this deep-sea fan system interacts with the Western Boundary Undercurrent adding to the complexity of this carbonate sedimentary system through its erosive power and by bringing large volume of clay-rich sediments originating far from the Canadian Provinces.

This study shows that carbonate gravity-flow systems can be comparable to siliciclastic turbidite systems. High-energy hydrodynamics in these systems can be provided by topographic chutes resulting from lithologic steps due to the vertical km-thick carbonate accumulation with different lithologies through long-term subsidence of long-lived carbonate platform such as the Exuma Platform. The heights of the chutes, linked to the carbonate platform unusually high reliefs, allows fast transfer of potential to kinetic energy, allowing the channelized flow to maintain a high competency and erosional power in the deposits located at the toe of the chutes. The unique high-slope gradient and, therefore, gravity force high potential, linked to the high constructive reliefs of long-lived carbonate platforms, compensate for the lack of flow momentum due to the absence of river input as in most siliciclastic systems. The unique high slope gradient also generates high competency and high capacity flows that can transport coarse-grained sediments that accumulate at the exit of those giant drainage carbonate systems on the adjacent abyssal plain and form deep sea fan with high-reservoir bearing capacity for hydrocarbons. Moreover, the occurrence of mass flow deposits and the formation of a large turbidite system at the mouth of the Exuma Valley/Canyon large carbonate drainage system suggests that, similar to what is known from siliciclastic canyons, mass-flow processes could also play a significant role in the occurrence and perhaps the genesis of such very-large valley/canyons in deep-water carbonate environments.

Acknowledgements

We thank the captain and crew of the R/V *L'Atalante* for the quality of the acquired data and Ifremer-Genavir for cruise organization and technical support. This work has been supported by the French Institute National des Sciences de l'Univers program “Actions Marges.” K. Fauquembergue PhD is funded by TOTAL. The two anonymous reviewers are deeply thanked for their valuable remarks on the early version of the manuscript.

References

- Austin, J.A., Schlager, W., et al., 1996. Proceedings Ocean Drilling Program Initial Reports: College Station. Ocean Drill. Program 101, pp. 501.
- Austin, J., Schlager, W., Palmer, A., Comet, P., Droxler, A., Eberli, G., Fourcade, E., Freeman-Lynde, R., Fulthorpe, C., Harwood, G., Kuhn, G., Lavoie, D., Leckie, M., Melillo, A., Moore, A., Mullins, H., Ravenne, C., Sager, W., Swart, P., Verbeek, J., Watkins, D., Williams, C., 1988. Proceeding Ocean Drilling Program, Scientific Results 101. College Station, TX. (501 pp.).
- Ball, M.M., 1967. Carbonate Sand Bodies of Florida and the Bahamas. *J. Sediment. Res.* 37 (2), 556–591.
- Benson, W.E., Sheridan, R.E., 1978. In: Benson, W.E., Sheridan, R.E., et al. (Eds.), Introduction and Principal Results. US. Government Printing Office, Washington, pp. 5–10.
- Benson, W.E., Sheridan, R.E., Enos, P., Freeman, T., Gradstein, F.M., Murdmaa, I.O., Pastouret, L., Schmidt, R.R., Stuermer, D.H., Weaver, F.M., Worstell, P., 1978. In: Benson, W.E., Sheridan, R.E., et al. (Eds.), Initial Reports of the Deep Sea Drilling Project, 44, Site 391: Blake Bahamas Basin. US. Government Printing Office, Washington, pp. 153–336.
- Bornhold, B.D., Pilkey, O.H., 1971. Bioclastic turbidite sedimentation in Columbus Basin, Bahamas. *Geol. Soc. Am. Bull.* 82, 1341–1354.
- Bulfinch, D.L., Ledbetter, M.T., Ellwood, B.B., Balsam, W.L., 1982. The high-velocity core of the Western Boundary Undercurrent at the base of the U.S. Continental Rise. *Science* 215, 970–973.
- Cartwright, R.A., 1985. Provenance and Sedimentology of Carbonate Systems From Two Deep-seas Fans, Bahamas (Ph.D. thesis). University of Miami, Miami, FL (114 p.).
- Cook, H.E., Egbert, R.M., 1981. Carbonate submarine fan facies along a Paleozoic prograding continental margin, western United States. *Am. Assoc. Pet. Geol. Bull.* 65, 913.
- Cook, H.E., McDaniel, P.N., Mountjoy, E.W., Pray, L.C., 1972. Allochthonous carbonate

- debris flows at Devonian bank ('reef') margins, Alberta, Canada. *Bull. Can. Petrol. Geol.* 20, 439–486.
- Corso, W.C., 1983. Sedimentology of rocks dredged from Bahamian platform slopes. Master Thesis. University of Florida, Miami, pp. 201.
- Crevello, P.D., Schlager, W., 1980. Carbonate debris sheet and turbidites, Exuma Sound, Bahamas. *J. Sediment. Res.* 50, 1121–1147.
- Droxler, A.W., 1984. Late Quaternary Glacial Cycles in the Bahamian Deep Basins and in the Adjacent Atlantic Ocean (Ph.D. thesis). University of Miami, Miami, FL (120 pp.).
- Droxler, A.W., Schlager, W., 1985. Glacial versus interglacial sedimentation rates and turbidite frequency in the Bahamas. *Geology* 13, 799–802.
- Droxler, A.W., Bruce, C.H., Sager, W.W., Watkins, D.H., 1988. Pliocene-Pleistocene variations in aragonite content and planktonic oxygen-isotope record in Bahamian periplatform ooze, Hole 633A. In: Austin Jr.J.A., Schlager, W., et al. (Eds.), *Proceeding Ocean Drilling Program, Scientific Results 101*. College Station, TX, pp. 221–244.
- Droxler, A.W., Mors, J.W., Glaser, K.S., Haddad, G.A., Baker, P.A., 1991. Surface Sediment Carbonate Mineralogy and Water Column Chemistry: Nicaragua Rise Versus the Bahamas Marine Geology. 100. pp. 277–289.
- Droz, L., Rigaut, F., Cochonat, P., Tofani, R., 1996. Morphology and recent evolution of the Zaire turbidite system (Gulf of Guinea). *Geol. Soc. Am. Bull.* 108, 253–269.
- Fabregas, N., 2018. Analyse de glissements sédimentaires sur la pente carbonatée d'Exuma Sound (Bahamas) à partir de données sismiques et bathymétriques (Master Thesis). Univ. Bordeaux (56 p.).
- Freeman-Lynde, R.P., Ryan, W.B.F., 1981. Erosional modification of Bahama Escarpment. *Geol. Soc. Am. Bull.* 96, 481–494.
- Freeman-Lynde, R.P., Cita, M.B., Jadoul, F., Miller, E.L., Ryan, W.B.F., 1981. Marine geology of the Bahama Escarpment. *Mar. Geol.* 44, 119–156.
- Gomes da Cruz, F.E., 2008. Processes, Patterns and Petrophysical Heterogeneity of Grainstone Shoals at Ocean Cay, Western Great Bahama Bank (Ph.D. Thesis). University of Miami, Miami, FL (244 p. Open Access Dissertations. Paper 180).
- Grammer, G.M., Ginsburg, R.N., Harris, P.M., 1993. Timing of deposition, diagenesis, and failure of steep carbonate slopes in response to a high-amplitude/high-frequency fluctuation in sea level, Tongue of the Ocean, Bahamas. In: Loucks, R.G., Sarg, J.F. (Eds.), *Carbonate Sequence Stratigraphy: Recent Developments and Applications*. American Association of Petroleum Geologists, Tulsa, OK, pp. 107–131.
- Haak, A.B., Schlager, W., 1989. Compositional variations in calciturbidites due to sea-level fluctuations, late Quaternary, Bahamas. *Geol. Rundsch.* 78, 477–486.
- Halley, R.B., Harris, P.M., Hine, A.C., 1983. Bank margin. In: Scholle, P.A., Bebout, D.G., Moore, C.H. (Eds.), *Carbonate Depositional Environments*. American Association of Petroleum Geologists Memoir 33. pp. 463–506 Chapter. 9.
- Harwood, G.M., Towers, P.A., 1988. Seismic sedimentological interpretation of a carbonate slope, north margin of Little Bahama Bank. In: *Proceeding Ocean Drilling Program Scientific Results*. 101. pp. 263–277.
- Heezen, B.C., Hollister, C.D., 1971. *The Face of the Deep*. Oxford University Press, London (659 pp.).
- Hine, A.C., 1983. Relict sand bodies and bedforms of the northern Bahamas: evidence of extensive early Holocene sand transport. In: Peryt, T.M. (Ed.), *Coated Grains*. Springer-Verlag, New York, pp. 116–131.
- Hine, A.C., Wilber, R.J., Bane, J., Neumann, A.C., Lorensen, K.R., 1981. Offbank transport of carbonate sands along open, leeward bank margins, northern Bahamas. In: Nittrouer, C.A. (Ed.), *Sedimentary Dynamics of Continental Shelves, Developments in Sedimentology*. 32. Elsevier, New York, pp. 327–348.
- Hollister, C.D., Ewing, J.I., Habib, D., Hathaway, J.C., Lancelot, Y., Luterbacher, H., Paulus, F.J., Poag, C.W., Wilcox, J.A., Worstell, P., 1972. Site 98: North East Providence channel; site 99: cat gap; site 100: cat gap; site 101: Blake Bahama Outer Ridge (southern end). In: Hollister, C.D., Ewing, J.I., et al. (Eds.), *Proceedings Deep Sea Drilling Program, Initial Reports, XI*. US Government Printing Office, Washington, pp. 9–134.
- Jo, A., Eberli, G.P., Grasmueck, M., 2015. Margin collapse and slope failure along southwestern Great Bahama Bank. *Sediment. Geol.* 317, 43–52.
- Joseph, P., Lomas, S., 2004. Deep-water sedimentation in the alpine foreland basin of the SE France: new perspectives on the Grès d'Annot and related systems—an introduction. In: Joseph, P., Lomas, S. (Eds.), *Deep-Water Sedimentation in the Alpine Foreland Basin of the SE France: New Perspectives on the Grès d'Annot and Related Systems*. Geological Society Special Publication 221. pp. 1–16.
- Kindler, P., Godefroid, F., Chiaradia, M., Ehler, C., Eisenhauer, A., Frank, M., Hasler, C.-A., Samankassou, E., 2011. Discovery of Miocene to early Pleistocene deposits on Mayaguana, Bahamas: evidence for recent active tectonism on the North American margin. *Geology* 39, 523–526. <https://doi.org/10.1130/G32011.1>.
- Komar, P.D., 1971. Hydraulic jumps in turbidity currents. *Geol. Soc. Am. Bull.* 82, 477–488.
- Kuhn, G., Meischner, D., 1988. Quaternary and Pliocene turbidites in the Bahamas Leg 101, sites 628, 632, and 635. In: Austin Jr.J.A., Schlager, W., et al. (Eds.), *Proceeding Ocean Drilling Program Scientific Results 101*. College Station, TX, pp. 203–212.
- Ladd, J.W., Sheridan, R.E., 1982. Cruise Report. C-2311. Bahama Carbonate Bank: Structure and Tectonics.
- Ladd, J.W., Sheridan, R.E., 1987. Seismic stratigraphy of the Bahamas. *AAPG Bull.* 71, 719–736.
- Land, L.A., Paull, C.K., Spiess, F.N., 1999. Abyssal erosion and scarp retreat: Deep Tow observations of the Blake Escarpment and Blake Spur. *Mar. Geol.* 160 (1–2), 63–83.
- Miall, A.D., 1985. Architectural-element analysis: a new method of facies analysis applied to fluvial deposits. *Earth Sci. Rev.* 22, 261–308.
- Migeon, S., Savoye, B., Zanella, E., Mulder, T., Faugères, J.-C., Weber, O., 2001. Detailed seismic-reflection and sedimentary study of turbidite sediment waves on the Var sedimentary Ridge (SE France): significance for sediment transport and deposition and for the mechanisms of sediment-waves construction. *Mar. Pet. Geol.* 18, 179–208.
- Mitchell, N.C., 2006. Morphologies of knickpoints in submarine canyons. *Geol. Soc. Am. Bull.* 118, 589–605.
- Mulder, T., Alexander, J., 2001. Abrupt change in slope causes variation in the deposit thickness of concentrated particle-driven density currents. *Mar. Geol.* 175, 221–235.
- Mulder, T., Ducassou, E., Gillet, H., Hanquiez, V., Tournadour, E., Combes, J., Eberli, G., Kindler, P., Gonthier, E., Conesa, G., Robin, C., Sianipar, R., Reijmer, J.J.G., François, A., 2012. Canyon morphology on a modern carbonate slope of the Bahamas: evidence of regional tectonic tilting. *Geology* 40, 771–774.
- Mulder, T., Joumes, M., Hanquiez, V., Gillet, H., Reijmer, J.J.G., Tournadour, E., Chabaud, L., Principaud, M., Schnyder, J., Borgomano, J., Fauquembergue, K., Ducassou, E., Busson, J., 2017. Carbonate slope morphology revealing sediment transfer from bank-to-slope (Little Bahama Bank, Bahamas). *Mar. Pet. Geol.* 83, 26–34.
- Mulder, T., Gillet, H., Hanquiez, V., Ducassou, E., Fauquembergue, K., Principaud, M., Conesa, G., Le Goff, J., Ragusa, J., Bashah, S., Bujan, S., Reijmer, J.J.G., Cavailles, T., Droxler, A.W., Blank, D.G., Guiastrrenec, L., Fabregas, N., Recouvreur, A., Seibert, C., 2018. Carbonate slope morphology revealing a giant submarine canyon (Little Bahama Bank, Bahamas). *Geology* 46 (1), 31–34.
- Mullins, H.T., Cook, H.E., 1986. Carbonate apron models: alternatives to the submarine fan model for paleoenvironmental analysis and hydrocarbon exploration. *Sediment. Geol.* 48, 37–79.
- Mullins, H.T., Hine, A.C., 1989. Scalloped bank margins: beginning of the end for carbonate platforms. *Geology* 17, 30–33.
- Mullins, H.T., Keller, G.H., Kofoed, J.W., Lambert, D.N., Stubblefield, W.L., Warme, J.E., 1982. Geology of Great Abaco submarine canyon (Blake Plateau): observations from the research submarine Alvin. *Mar. Geol.* 48, 239–257.
- Mullins, H.T., Heath, K.C., van Buren, H.M., Newton, C.R., 1984. Anatomy of a modern open-ocean carbonate slope: Northern Little Bahama Bank. *Sedimentology* 31, 141–168.
- Mutti, E., 1977. Distinctive thin-bedded turbidites facies and related depositional environments in the Eocene Hecho Group (South-central Pyrenees, Spain). *Sedimentology* 24, 107–131.
- Normark, W.R., 1970. Growth patterns of deep-sea fans. *Am. Assoc. Pet. Geol. Bull.* 54, 2170–2195.
- Normark, W.R., Piper, D.J.W., Hess, G.R., 1979. Distributary channels, sand lobes, and mesotopography of navy submarine fan, California Borderland, with application to ancient fan sediments. *Sedimentology* 26, 749–774.
- Paull, C.K., Dillon, W.P., 1980. Erosional origin of the Blake Escarpment: an alternative hypothesis. *Geology* 8, 538–542.
- Paull, C.K., Neumann, A.C., 1987. Continental margin brine seeps: their geological consequences. *Geology* 15, 545–548.
- Payros, A., Pujalte, V., 2008. Calciastic submarine fans: an integrated overview. *Earth Sci. Rev.* 86, 203–246.
- Playton, T., Janson, X., Kerans, C., 2010. 18. Carbonate Slopes. In: James, N.P., Dalrymple, R.W. (Eds.), *Facies*. 4. Geological Association of Canada, St. John's, Newfoundland, pp. 449–476.
- Rankey, E.C., Doolittle, D.F., 2012. Geomorphology of carbonate platform-marginal up-permost slopes: insights from a Holocene analogue, Little Bahama Bank, Bahamas. *Sedimentology* 59, 2146–2171. <https://doi.org/10.1111/j.1365-3091.2012.01338.x>.
- Rankey, E.C., Enos, P., Steffen, K., Druke, D., 2004. Lack of impact of hurricane Michelle on tidal flats, Andros Island, Bahamas: integrated remote sensing and field observations. *J. Sediment. Res.* 74 (5), 654–661.
- Rankey, E.C., Riegl, B., Steffen, K., 2006. Form, function and feedbacks in a tidally dominated ooid shoal, Bahamas. *Sedimentology* 53, 1191–1210.
- Ravenne, C., 2002. Stratigraphy and oil: a review. Part 1. Exploration and seismic stratigraphy: observation and description. *Oil Gas Sci. Technol. Rev. I'IFP* 57, 211–250.
- Ravenne, C., Le Quéllec, P., Valery, P., 1985. Dépôts carbonatés profonds des Bahamas. In: Géodynamique des Caraïbes. Symposium, TECHNIP, Paris, France, pp. 255–270.
- Reading, H.G., Richard, M.T., 1994. The classification of deep-water siliciclastic depositional systems by grain size and feeder systems. *Am. Assoc. Pet. Geol. Bull.* 78, 792–822.
- Reeder, S.L., Rankey, E.C., 2008. Interactions between tidal flows and ooid shoals, Northern Bahamas. *J. Sediment. Res.* 78 (3), 175–186.
- Reeder, S.L., Rankey, E.C., 2009a. Controls on morphology and sedimentology of carbonate tidal deltas, Abacos, Bahamas. *Mar. Geol.* 267, 141–155.
- Reeder, S.L., Rankey, E.C., 2009b. A tale of two storms: and integrated field, remote sensing, and modeling study examining the impact of hurricanes Frances and Jeanne on carbonate systems, Bahamas. In: Swart, P.K., Eberli, G.P., McKenzie, J.A. (Eds.), *Perspectives in Carbonate Geology: A Tribute to the Career of Robert Nathan Ginsburg*. John Wiley & Sons, Ltd., pp. 75–90.
- Reijmer, J.J.G., Schlager, W., Droxler, A.W., 1988. Site 632: Pliocene-Pleistocene sedimentation cycles in a Bahamian basin. In: Austin Jr.J.A., Schlager, W., et al. (Eds.), *Proceeding Ocean Drilling Program, Scientific Results 101*, College Station (TX), pp. 213–220.
- Reijmer, J.J.G., Schlager, W., Bosscher, H., Beets, C.J., McNeill, D.F., 1992. Pliocene/Pleistocene platform facies transition recorded in calciturbidites (Exuma Sound, Bahamas). *Sediment. Geol.* 78, 171–179.
- Reijmer, J.J.G., Palmieri, P., Groen, R., 2012. Compositional variations in calciturbidites and calclitebrites in response to sea-level fluctuations (Exuma Sound, Bahamas). *Facies* 58, 493–507.
- Reijmer, J.J.G., Mulder, T., Borgomano, J., 2015a. Carbonate slope and gravity deposits. *Sediment. Geol.* 317, 1–8.
- Reijmer, J.J.G., Palmieri, P., Groen, R., Floquet, M., 2015b. Calciturbidites and calclitebrites: sea-level variations or tectonic processes? *Sediment. Geol.* 317, 53–70.
- Rendle-Bühning, R.H., Reijmer, J.J.G., 2005. Controls on grain-size patterns in

- periplatform carbonates: marginal setting versus glacio-eustasy. *Sediment. Geol.* 175, 99–113.
- Schlager, W., Chermak, A., 1979. Sediment facies of platform-basin transition, Tongue of the Ocean, Bahamas. In: *Society of Economic Paleontologists and Mineralogists (Society for Sedimentary Geology) Special Publication*. 27. pp. 193–208.
- Schlager, W., Ginsburg, R.N., 1981. Bahama carbonate platforms — the deep and the past. *Mar. Geol.* 44, 1–24. [https://doi.org/10.1016/0025-3227\(81\)90111-0](https://doi.org/10.1016/0025-3227(81)90111-0).
- Schlager, W., Austin Jr., J.A., Corso, W., McNulty, C.L., Flügel, E., Renz, O., Steinmetz, J.C., 1984. Early Cretaceous platform reentrant and escarpment erosion in the Bahamas. *Geology* 12, 147–150.
- Schmitt, A., 2013. Etude des processus de dépôt des marges carbonatées dans les Bahamas: Exemple du petit banc des Bahamas et de San Salvador (MSc thesis). University of Bordeaux (48 pp.).
- Shanmugam, G., Moiola, R.J., McPherson, J.G., O'Connell, S., 1988. Comparison of modern Mississippi fan with selected ancient fans. *Trans. Gulf Coast Assoc. Geol. Soc.* 38, 157–165.
- Sheridan, R.E., Crosby, J.T., Bryan, G.M., Stoffa, P.L., 1981. Stratigraphy and structure of southern Blake Plateau, northern Florida Straits, and northern Bahama Platform from multichannel seismic reflection data. *AAPG Bull.* 65, 2571–2593.
- Sheridan, R.E., Mullins, H.T., Austin, J.J.A., Ball, M.M., Ladd, J.W., 1988. Geology and geophysics of the Bahamas. In: Sheridan, R.E., Grow, J.A. (Eds.), *The Geology of North America Volume 1–2, The Atlantic Continental Margin*. Geological Society of America, U.S.
- Soulet, Q., Migeon, S., Gorini, C., Rubino, J.-L., Raison, F., Bourges, P., 2016. Erosional versus aggradational canyons along a tectonically-active margin: the northeastern Ligurian margin (western Mediterranean Sea). *Mar. Geol.* 382, 17–36.
- Spence, G.H., Tucker, M.E., 1997. Genesis of limestone megabreccias and their significance in carbonate sequence stratigraphic models: a review. *Sediment. Geol.* 112 (163), 193.
- Stow, D.A.V., Hernández-Molina, F.J., Llave, E., Sayago-Gil, M., Díaz Del Río, V., Branson, A., 2009. Bedform-velocity matrix: the estimation of bottom current velocity from bedform observations. *Geology* 37, 327–330. <https://doi.org/10.1130/G25259A>.
- Thomas, D.J., Via, R.K., 2007. Neogene evolution of Atlantic thermohaline circulation: Perspective from Walvis Ridge, southeastern Atlantic Ocean. *Paleoceanography* 22 (2), PA2212. <https://doi.org/10.1029/2006PA001297>.
- Tournadour, E., 2015. Architecture et dynamique sédimentaire d'une pente carbonatée moderne: exemple de la pente Nord de Little Bahama Bank (LBB), Bahamas (Ph.D. Thesis). University of Bordeaux (300 p.).
- Wilber, R.J., Milliman, J.D., Halley, R.B., 1990. Accumulation of bank-top sediment on the western slope of Great Bahama Bank: rapid progradation of a carbonate megabank. *Geology* 18, 970–974. [https://doi.org/10.1130/0091-7613\(1990\)018<0970:AOBTSO>2.3.CO;2](https://doi.org/10.1130/0091-7613(1990)018<0970:AOBTSO>2.3.CO;2).
- Wunsch, M., Betzler, C., Lindhorst, S., Lüdmann, T., Eberli, G.P., 2016. Sedimentary dynamics along carbonate slopes (Bahamas archipelago). *Sedimentology* 64 (3), 631–657.
- Wunsch, M., Betzler, C., Eberli, G.P., Lindhorst, S., Lüdmann, T., Reijmer, J.J.G., 2018. Sedimentary dynamics and high-frequency sequence stratigraphy of the southwestern slope of Great Bahama Bank. *Sediment. Geol.* 363, 96–117.
- Wynn, R.B., Kenyon, N.H., Masson, D.G., Stow, D.A.V., Weaver, P.P.E., 2002. Characterization and recognition of deep-water channel-lobe transition zones. *Am. Assoc. Pet. Geol. Bull.* 86, 1441–1446.